Available online at www.sciencedirect.com

SCIENCE DIRECT®

ELSEVIER

Palaeogeography, Palaeoclimatology, Palaeoecology 228 (2005) 338–360

PALAEO

www.elsevier.com/locate/palaeo

Late Pliocene climate variability on Milankovitch to millennial time scales: A high-resolution study of MIS100 from the Mediterranean

Julia Becker *, Lucas J. Lourens, Frederik J. Hilgen, Erwin van der Laan, Tanja J. Kouwenhoven, Gert-Jan Reichart

Department of Stratigraphy–Paleontology, Faculty of Earth Sciences, Utrecht University, Budapestlaan 4, 3584 CD Utrecht, Netherlands

Received 10 November 2004; received in revised form 19 June 2005; accepted 22 June 2005

Abstract

Astronomically tuned high-resolution climatic proxy records across marine oxygen isotope stage 100 (MIS100) from the Italian Monte San Nicola section and ODP Leg 160 Hole 967A are presented. These records reveal a complex pattern of climate fluctuations on both Milankovitch and sub-Milankovitch timescales that oppose or reinforce one another. Planktonic and benthic foraminiferal $\delta^{18}O$ records of San Nicola depict distinct stadial and interstadial phases superimposed on the saw-tooth pattern of this glacial stage. The duration of the stadial–interstadial alterations closely resembles that of the Late Pleistocene Bond cycles. In addition, both isotopic and foraminiferal records of San Nicola reflect rapid changes on timescales comparable to that of the Dansgard–Oeschger (D–O) cycles of the Late Pleistocene. During stadial intervals winter surface cooling and deep convection in the Mediterranean appeared to be more intense, probably as a consequence of very cold winds entering the Mediterranean from the Atlantic or the European continent.

The high-frequency climate variability is less clear at Site 967, indicating that the eastern Mediterranean was probably less sensitive to surface water cooling and the influence of the Atlantic climate system. Concomitant changes in the colour reflectance of ODP Site 967 and the calcium carbonate record of San Nicola probably indicate that part of the high-frequency climate variability (3–5 kyr) in the eastern Mediterranean is related to changes in Saharan dust supply. Evidently, enhanced dust deposition in the Mediterranean correlates with the cold intervals of the millennial-scale D–O oscillations suggesting that the Atlantic pressure system may have played a critical role in varying the wind strength and/or aridification of northern Africa.

Keywords: Mediterranean; Pliocene; Planktonic foraminifera; Benthic foraminifera; Stable isotopes

* Corresponding author. Fax: +31 30 2532648.
E-mail address: becker@geo.uu.nl (J. Becker).

0031-0182/$ - see front matter © 2005 Elsevier B.V. All rights reserved.
doi:10.1016/j.palaeo.2005.06.020

1. Introduction

Much work has been done in describing and modelling natural variability of the Earth's climate system. While it has been demonstrated that variations in the Earth's climate system at Milankovitch timescales (20 to 400-kyr) are caused by variations in the solar insolation and, hence, are orbitally induced, the origin of climate variability at sub-Milankovitch timescales (periods<20-kyr) is still under debate. Possible forcing mechanisms that have been proposed for these high-frequency climate variations include non-linear response to harmonics or combination tones of the main orbital cycles (Pestiaux et al., 1988; Hagelberg et al., 1994; Ortiz et al., 1999), twice-yearly overhead passage of the sun across the equator (Short and Mengel, 1986; Short et al., 1991), variation in solar output (Van Geel et al., 1999; Perry and Hsu, 2000; Bond et al., 2001) or periodic motion of the Earth and Moon (Keeling and Whorf, 2000).

From sedimentary and ice-core data it became evident that the Earth's climate system is extremely instable, especially during the last glacial. Rapid cold–warm fluctuations in North Atlantic sea surface and Greenland air temperature are associated with fluctuations in global thermohaline circulation and occasionally with ice rafting events from Northern Hemisphere ice sheets (Heinrich, 1988; Bond, 1992; Bond et al., 1993, 1999; Dansgaard et al., 1993). The occurrence of high-amplitude millennial-scale climate variations during full glacial conditions in contrast to relatively low-amplitude millennial-scale variability during interglacial times (e.g., Holocene) suggests that Northern Hemisphere ice sheets are important. However, the role of large ice sheets is still controversial, because some models propose ice sheets to be the trigger for tropical climate variability (MacAyeal, 1993), whereas others argue that rapid oscillations of the northern climate are a response to rather than the cause of low latitude climate variability (McIntyre and Molfino, 1996; Curry and Oppo, 1997). Proposed mechanisms are those including changes in the equatorial wind system equivalent to long-term changes in El Niño- Southern Oscillation (ENSO) and changes in the intensity of the Inter Tropical Convergence Zone (ITCZ) and monsoon variability (Stott et al., 2002). Moreover, older records show that high-frequency variability is a significant component of high-latitude and low-latitude climate prior to the onset of Northern Hemisphere glaciations (Ortiz et al., 1999; Steenbrink et al., 2003). Although the interpretation of these records is not straightforward they strengthen the idea that high-frequency components are persistent in the Earth's climate and independent from the large ice sheets of the Late Pleistocene. But it is generally accepted that northern Hemisphere ice sheets (or possibly even southern Hemisphere ice sheets) act as amplifiers (Raymo et al., 1992; McIntyre et al., 2001) or a resonating system (Wara et al., 2000).

Most studies on millennial-scale climate variability have focussed on the Late Pleistocene time interval when glacial–interglacial alternations were primarily paced by the 100-kyr periodicity (Imbrie et al., 1993), of which the origin has been intensively debated (Le Treut and Ghil, 1983; Imbrie et al., 1984, 1992; Saltzman and Sutera, 1984; Liu, 1992, 1995; Clemens and Tiedemann, 1997; Rial, 1999; Shackleton, 2000). In contrast, it is generally accepted that the glacial–interglacial cycles of the Late Pliocene and Early Pleistocene are controlled by the obliquity cycle (Shackleton et al., 1984; Ruddiman et al., 1986; Raymo et al., 1989). Hence studying these glacial–interglacial cycles in high resolution may shed new light upon the relation between millennial-scale and astronomically-driven climate cycles. Here, we present a high-resolution multi-proxy study of the Late Pliocene marine oxygen isotope stage 100 (MIS100) from the Mediterranean to unravel millenial-scale climate variability in a region that is well known to

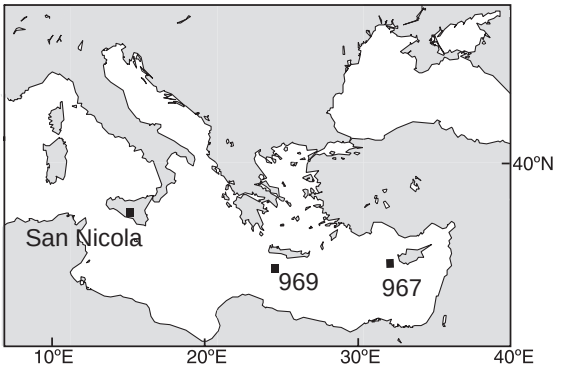

Fig. 1. Location map.

be dominated by the Earth's precession and obliquity cycles throughout the Late Neogene (i.e. Lourens et al., 1992, 1996; Hilgen et al., 1995). MIS100 was chosen as case study, because in the first place it revealed characteristic high-frequency changes in sediment colour in both the land-based marine succession Monte San Nicola (Sicily, Italy) and ODP Site 967 (Figs. 1 and 2). Secondly, both sequences have been astronomically calibrated, independent of global ice volume chronologies (Lourens et al., 2001, 2004). Finally, MIS100 is one of the first pronounced obliquity-controlled glacial periods at the onset of Northern Hemisphere glaciations (Shackleton et al., 1984; Raymo et al., 1989). Evidence for occasional massive discharge of icebergs during these first full glacial cycles comes from ice rafted debris (IRD) records in DSDP/ODP cores from the North Atlantic (Raymo et al., 1992; Carter and Raymo, 1999). Rapid changes in the size of the continental ice-sheets at that time are confirmed by major shifts in benthic

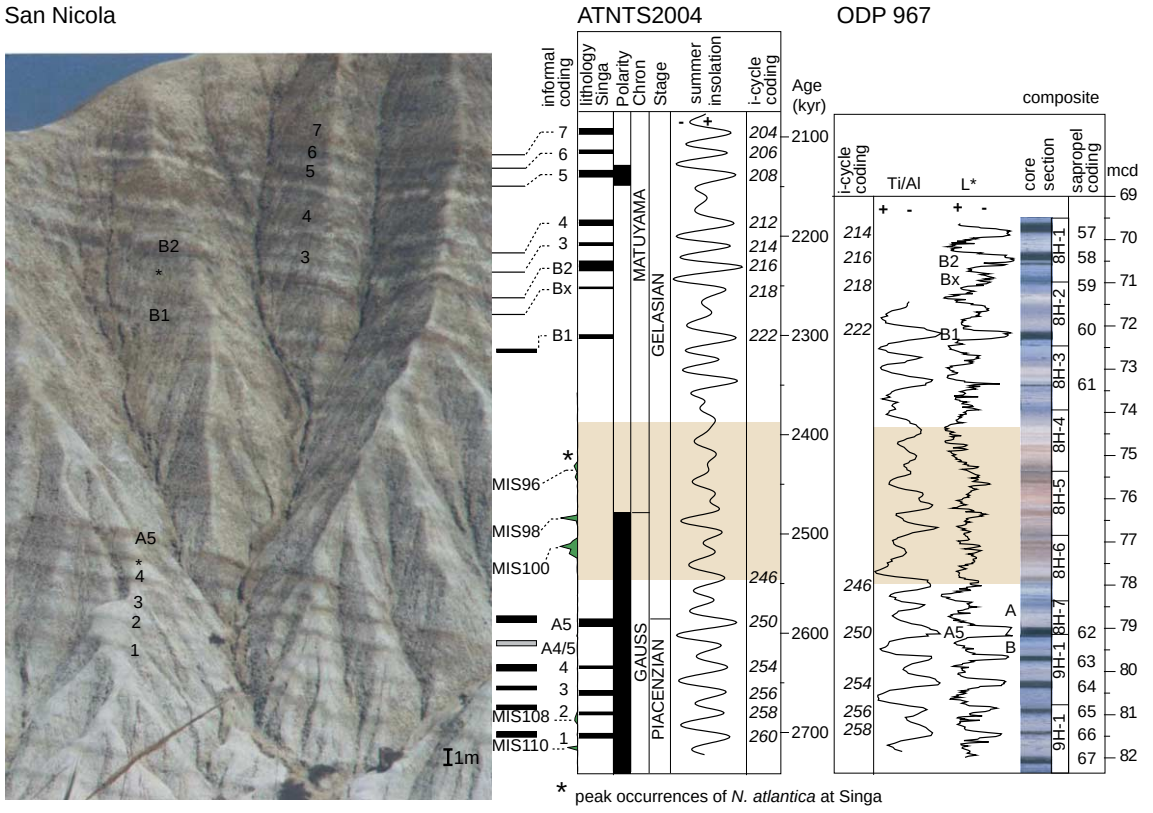

Fig. 2. Lithology of Monte San Nicola section in comparison with the ATNTS2004 and lithology of ODP Site 967. Individual sapropels of sapropel clusters A and B (informal coding after Verhallen, 1987; Zijderveld et al., 1991) are labelled in the photograph of SN. Thick black and grey bars at the right hand side of the photograph indicate stratigraphic positions (scale bar lower right corner) of sapropels as recorded by Hilgen et al., (1991) and thin bars indicate positions of sapropels as assumed from the photograph. Stipple lines indicate correlation to the lithology of the Monte de Singa section as incorporated in the ATNTS2004 (Lourens et al., 2004). Additionally, marine isotope stages (MIS) 110, 108 and 100–96 are indicated in the lithology of SN and by peak occurrences of *Neogloboquadrina atlantica* (green shaded) at Singa (Lourens et al., 1992). The ATNTS2004 shows the sapropel occurrences, polarity, chrons, stages in relation to the $La04_{(1,1)}$ 65°N summer insolation curve. Insolation maxima correlating to sapropels are labelled according to the i-cycle coding after Hilgen et al., (1991) and ages (kyr) are indicated on the right axis. The yellow shaded area indicates the interval of MIS101-95. Ti/Al, colour reflectance and lithology of ODP leg 160 Site 967 (composite) are plotted versus meter composite depth (mcd), after Sakamoto et al. (1998). I-cycle codes are indicated on the left and sapropel codes of Kroon et al. (1998) on the right. Sapropels A5, B1, Bx and B2 are indicated in addition. The yellow shaded area indicates the interval of MIS101-95. (For interpretation of the references to colour in this figure legend, the reader is referred to the web version of this article.)

foraminiferal oxygen isotope records (Raymo et al., 1989, 1992).

2. Material and methods

Monte San Nicola is situated 10 km north of the coastal town Gela in southern Sicily (Italy) (for detailed location map and description see (Rio et al., 1994)). A succession of ~160 m of rhythmically bedded marly limestones and marls from the Trubi and Monte Narbone Formation are well exposed. The sapropels of the O, A, B and C clusters (Verhallen, 1987; Zijderveld et al., 1991) are visible in the section (Fig. 2). The sedimentary sequence was estimated to be deposited at a water depth of 800–1000 m (Bonaduce and Sprovieri, 1984; Rio et al., 1994) with an average sedimentation rate of ~8 cm/kyr (Sprovieri et al., 1986). The section presents the Gelasian stratotype (Rio et al., 1994) with the base of the Gelasian being defined at the top of the A5 sapropel (Fig. 2).

Monte San Nicola has been used to establish the astronomically calibrated (polarity) timescale by Hilgen (Hilgen, 1991a,b). The position of marine oxygen isotope stages (MIS) 96–100 is well constrained in this section (Sprovieri, 1993). These stages are visible as grey-white alternations on a metre scale in-between the A5 sapropel and the B sapropel group with grey layers reflecting glacial stages 100, 98 and 96 (Fig. 2). Light-coloured decimetre thick bands are visible within the dark glacial stages. The base of MIS101 is characterised by a dark layer which is a not fully developed sapropel (ghost sapropel) corresponding to i-cycle 246 (Lourens et al., 1996).

The MIS101 to MIS99 interval was sampled every 3 cm. The sampling trajectory was chosen carefully to ensure a continuous and undisturbed record. The weathered surface was cleaned and only 'fresh' material was sampled. Generally, two cores of 2.5 cm diameter were drilled per sample level using an electric water-cooled drill. Samples for foraminiferal counts and stable isotope analysis were dried at 50 °C in an oven and were washed through 63, 125 and 600 μm sieves. Samples for geochemical analysis were dried and homogenised in an agate mortar.

ODP Leg 160 Site 967 (34°04′N, 32°43′E) was drilled in the eastern Mediterranean near the Eratosthenes seamount at a water depth of 2554 m. The palaeodepth was estimated to be 1800–2500 m (Emeis et al., 1996). Three holes were drilled in order to gain a continuous succession. A composite depth profile was constructed by correlating colour reflectance records between different holes (Sakamoto et al., 1998). The top 125 m consist of Lower Pliocene to Holocene hemipelagic sediments containing 80 sapropels. Sapropels occur in clusters and correlate to the large-scale sapropel groups O, A, B and C as exposed in the land-based marine successions of the Vrica, Singa, Punta Piccola and San Nicola sections (Kroon et al., 1998; Lourens et al., 1998). The interval between the A5 sapropel and the B sapropel group is marked by a reddish colour and glacial stages 100, 98 and 96 are visibly darker in the core (Fig. 2). Hole A on Site 967 was sampled every centimetre in the interval 8H4–6 (hereafter referred to as Site 967). Core photographs and colour reflectance data of all holes (A–C) were used to check the stratigraphic completeness and undisturbance of the core section. Additionally, colour reflectance was measured on the half core every centimetre and on the individual samples using a hand-held Minolta CM 503i spectrophotometer. Samples for foraminiferal stable isotope analysis were freeze-dried and washed through 63, 125 and 600 μm sieves.

For stable isotope analysis of the San Nicola samples about 20 specimens of the benthic foraminifer *Uvigerina peregrina* and 50 specimens of the planktonic foraminifer *Globigerinoides ruber* were hand picked from a split of the >212 μm size fraction in the size range 300–400 μm. The analysis was carried out at Utrecht University stable isotope facility where an ISOCARB common bath carbonate preparation device linked on-line to a VG SIRA24 mass spectrometer is operated. Isotope values were calibrated to the PeeDeeBelemnite (PDB) scale. Analytical precision was determined by replicate analyses and by comparison to the international (IAEA-CO1) and in house carbonate standard (NAXOS). Replicate analyses showed standard deviations of <0.06‰ and <0.1‰ for $\delta^{13}C$ and $\delta^{18}O$, respectively.

For benthic stable isotope analysis of Site 967 3–5 specimens of *Cibicidoides kullenbergi* were hand picked from the >212 μm fraction in the size range 300–400 μm. Measurements were carried out at Bremen University stable isotope facilities where a CARBO-KIEL automated carbonate preparation device linked on-line to a FINNIGAN MAT 251

mass spectrometer is operated. Replicate analyses and calibration to the international carbonate standard NBS19 and in-house standard (shk_br; carrara) revealed an analytical precision better than 0.03‰ and 0.05‰ for $\delta^{13}C$ and $\delta^{18}O$, respectively. The $\delta^{18}O$ results of *C. kullenbergi* were adjusted by adding 0.64‰ to be in equilibrium with *Uvigerina* and ambient sea water (Shackleton, 1974).

Carbon weight percentages were measured before and after removal of carbonates with 1 M HCl on a Fisons Instruments NCS NA 1500 analyser (Utrecht University) using dry-combustion at 1030 °C. Relative standard deviations in duplicate measurements are below 3‰ for carbon and 4‰ for nitrogen. Carbonate weight percentages were calculated by converting all inorganic carbon into carbonate.

Quantitative foraminiferal analysis was carried out on the San Nicola samples by counting approximately 200 specimens per sample from splits of the >125 μm size fraction. Splits were obtained using an Otto

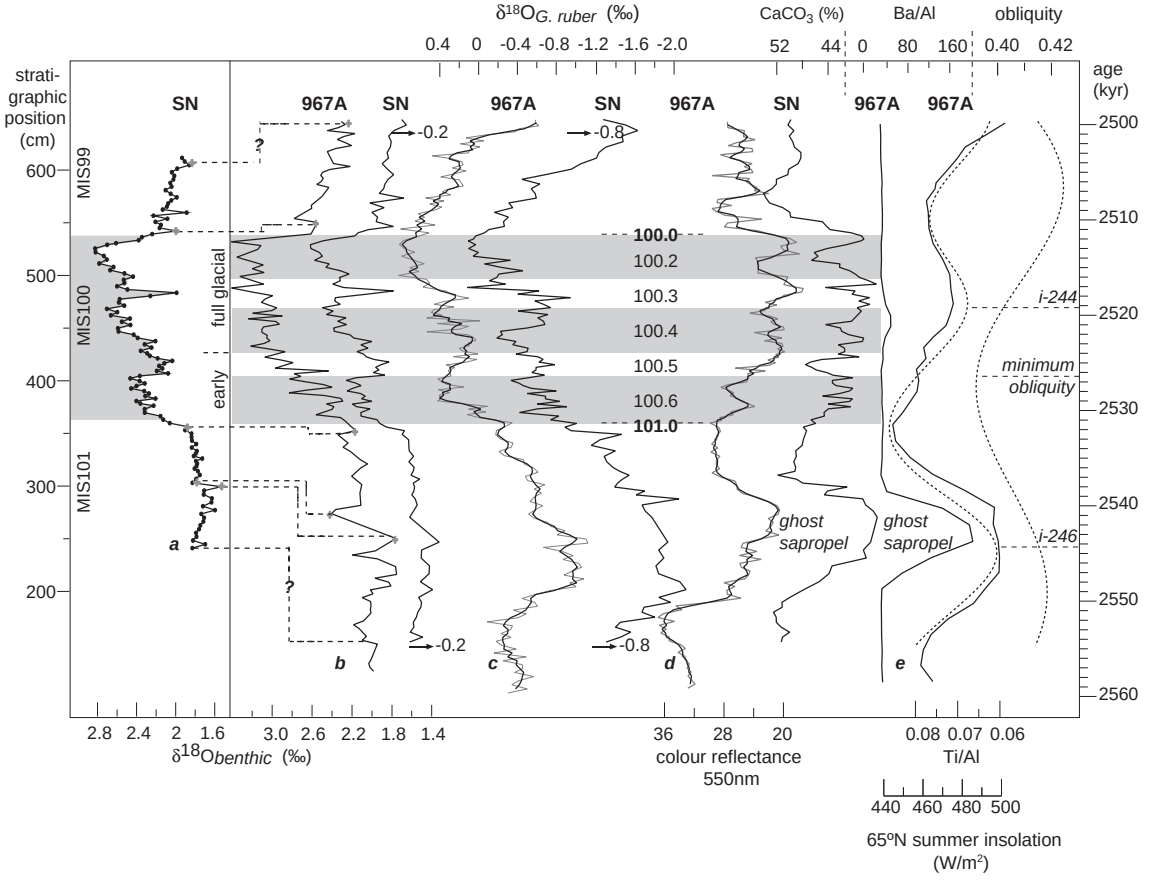

Fig. 3. a) Graphical correlation of the $\delta^{18}O_{benthos}$ record of San Nicola (versus depth) with the $\delta^{18}O_{benthos}$ of ODP Site 967A (versus age). Crosses and stippled lines indicate tie points used for age calibration. Ages are interpolated linearly in between tie points. b) $\delta^{18}O_{benthos}$ of San Nicola versus age plotted on the same (inversed) *x*-axis as $\delta^{18}O_{benthos}$ of Site 967. Shaded areas indicate stadials with even labels referring to stadials and odd labels referring to interstadials, respectively. Marine oxygen isotope stage 100 extends from 2531.5 to 2511.5 kyr. The distribution into an early and full glacial phase is indicated on the right age-axis. c) $\delta^{18}O_{plankton}$ curves of ODP Site 967A and San Nicola plotted on common axes (inverse *x*-axis). Note that the San Nicola curve is shifted 0.8‰ towards lighter values for clarity. A three point moving average (dark line) overlies the $\delta^{18}O_{plankton}$ of site 967A d) ODP Site 967A 550 nm colour reflectance (dark line) with superimposed three point moving average and San Nicola bulk sediment $CaCO_3$ weight percentage. Low values in the colour reflectance and $CaCO_3$ weight percentage respectively mark the position of the ghost sapropel. d) ODP Site 967A Ba/Al, Ti/Al (inversed) (data from Lourens et al., 2001) and Laskar04$_{(1,1)}$ 65°N summer insolation (stipple-line) and obliquity. I-cycles i-246 and i-244 (i-cycle notation after Lourens et al., 1996) are indicated on the left age-axis.

micro-splitter. All specimens were picked, mounted on Chapman slides and identified. The juvenile forms of the planktonic species *Globigerina falconensis* and *Globigerina bulloides* were counted together because of their close morphological similarity. The adult forms are predominantly specimens of *G. falconensis* and very few specimens of *G. bulloides* and, therefore, plotted together. Sinistrally and dextrally coiled forms of the *Neogloboquadrina* sp. group were counted separately. In the benthic foraminiferal group of the non-costate buliminids *Bulimina aculeata* s.s., *Bulimina marginata* s.s. and intermediate morphotypes are counted together. Groups like miliolids, discorbids, nodosariidae and *Elphidium* spp. are not specified any further.

2.1. Age model

The studied interval of ODP Site 967 has been astronomically dated by correlating the Ti/Al to the $La90–93_{(1,0.5)}$ 65°N summer insolation curve (Lourens et al., 2001). The Ti/Al ratio has been interpreted in terms of changes in the relative contribution of aeolian versus fluvial material. For statistical purposes Lourens et al. (2001) assumed an in-phase relationship between Ti/Al and 65°N summer insolation. Therefore, ages of i-cycle 246 and 244 differ by 3 kyr from the lagged ages given by Lourens et al. (1996). Here, we apply a new astronomical solution, $La04_{(1,1)}$ with present-day values for the Earth's tidal dissipation and dynamical ellipticity (Laskar et al., 2004) in stead of the older La90–93 solution (Laskar et al., 1993), although both solutions reveal the same ages within the studied interval.

The age model for San Nicola is based on the graphical correlation between the benthic oxygen isotope record of San Nicola and Site 967 (Fig. 3a). Tie-points were set at the MIS101/MIS100 and MIS100/MIS99 transitions and within MIS99 and MIS101. Ages in between the tie-points are interpolated linearly resulting in a duration of ~20 kyr for MIS100 and average sedimentation rates of ~6 and ~8.6 cm/kyr equivalent to a time resolution of ~500 and ~350 yr in the interglacials and the glacial of San Nicola, respectively. Sedimentation rate at Site 967 is on average 2.5 cm/kyr, resulting in a sample resolution of ~400 yr.

3. Results

3.1. Oxygen isotopes

San Nicola $\delta^{18}O$ values for *U. peregrina* ($\delta^{18}O_{benthos}$) and *G. ruber* ($\delta^{18}O_{G.ruber}$) are highest during MIS100 with maximum values being 2.8‰ and 0.8‰, respectively (Fig. 3b,c). Lowest values (−1.2‰ for $\delta^{18}O_{G.ruber}$ and 1.6‰ for $\delta^{18}O_{benthos}$) are reached during the ghost sapropel. Average interglacial $\delta^{18}O_{benthos}$ values (MIS99 and MIS101 averaged) are 1.8‰ resulting in a glacial–interglacial (G–I) difference (maximum–average interglacial) of ~1.0‰ for $\delta^{18}O_{benthos}$. Interglacial $\delta^{18}O_{G.ruber}$ values are ~−0.6‰ during MIS101 except for the ghost sapropel and decrease from maximum glacial values of −1.2‰ to minimum interglacial values of −0.6‰ during MIS99. The $\delta^{18}O_{G.ruber}$ values decrease later and slower than $\delta^{18}O_{benthos}$ values (Fig. 3b). At the MIS100/MIS99 transition $\delta^{18}O_{benthos}$ is already ~3/4 the interglacial value, whereas $\delta^{18}O_{G.ruber}$ is still at one third the interglacial value. Assuming a minimum interglacial $\delta^{18}O_{G.ruber}$ value of ~−0.6‰, a value that is reached at the beginning of MIS101, before the MIS101/100 transition and at the top of the record in MIS99 results in a G–I difference (maximum glacial–assumed interglacial) of ~1.4‰ for $\delta^{18}O_{G.ruber}$.

Benthic oxygen isotope values of Site 967 are generally ~0.5‰ heavier than at San Nicola, except during the onset of MIS100, averaging to 2.2‰ in the interglacial and ~3.2‰ in the glacial. This implies that the glacial–interglacial $\delta^{18}O_{benthos}$ difference of Site 967 is like at San Nicola 1.0‰. This is in close agreement with G–I amplitudes of North Atlantic records (Ruddiman et al., 1986; Raymo et al., 1989; Lisiecki and Raymo, 2005). Lowest $\delta^{18}O_{G.ruber}$ values (−1.0‰) of Site 967 are associated with the ghost sapropel, being ~−0.3‰ before and after the sapropel, a value that is also reached at the top of MIS99 and during the following interglacials (unpublished data). Therefore, interglacial $\delta^{18}O_{G.ruber}$ values of Site 967 are assumed to be in the range of −0.3‰ and thus heavier by 0.3‰ than interglacial $\delta^{18}O_{G.ruber}$ values of San Nicola. This results in a G–I (maximum glacial–assumed interglacial) $\delta^{18}O_{G.ruber}$ difference of ~1.1‰ for Site 967 compared to 1.4‰ for at San Nicola. Furthermore, $\delta^{18}O_{G.ruber}$ values of Site 967 decrease also much slower after the MIS100/99 tran-

sition than associated $\delta^{18}O_{benthos}$. Planktonic and benthic oxygen isotope records of both sites show a remarkable good correlation (Table 1) revealing an overall distinct saw-tooth pattern characterised by a gradual increase during the early glacial towards maximum values during full glacial conditions and a sudden decrease at the termination. A time lag of ~8 kyr can be observed between the midpoint of MIS100 (~2.519 Ma) and the minimum in obliquity at 2.527 Ma (Fig. 3e).

The $\delta^{18}O_{benthos}$ record of San Nicola is furthermore characterised by three sub-cycles. Each sub-cycle shows a saw-tooth pattern, starting with a gradual increase in isotope values that takes about 4–5 kyr followed by a sudden decrease to lighter values. Values remain low for another 2–3 kyr so that the average duration of each sub-cycle is 6–8 kyr. We labelled the San Nicola sub-stages according to the nomenclature established for Late Pleistocene glacials where even numbers refer to stadial phases and odd numbers refer to interstadial phases (Imbrie et al., 1984; Martinson et al., 1987). San Nicola sub-stages are also observed in the $\delta^{18}O_{G.ruber}$, but are generally noisier. Benthic and planktonic $\delta^{18}O$ values correlate except for the stadial MIS100.4 where the relation is partly inversed. Sub-stages have amplitudes of about 0.4–0.5‰. Partitioning into an early and a full glacial is also evident in the $\delta^{18}O_{benthos}$ of Site 967, but sub-stages as defined in San Nicola are not clear. Millennial-scale (2–3 kyr) variations in the order of 0.2–0.4‰ can be recognised in both $\delta^{18}O_{benthos}$ records.

Table 1
Correlation coefficients between selected parameters of SN and Site 967

r	Site 967 $\delta^{18}O_{benthos}$	SN $\delta^{18}O_{G.ruber}$	SN $\delta^{18}O_{benthos}$	SN $CaCO_3$
Site 967	0.85	0.94	0.88	n.s.
$\delta^{18}O_{G.ruber}$	$(0.58)_1$	(0.76)	(0.67)	(−0.37)
Site 967		0.86	0.91	−0.29
$\delta^{18}O_{benthos}$		(0.55)	(0.63)	(−0.42)
SN			0.88	n.s.
$\delta^{18}O_{G.ruber}$			(0.61)	(−0.30)
SN				−0.26
$\delta^{18}O_{benthos}$				(−0.44)
Site 967	−0.58	−0.37	−0.49	0.64
CR	(−0.85)	(−0.47)	(−0.53)	(0.36)

1) Numbers in brackets are coefficients for MIS100 only.

3.2. Calcium carbonate

$CaCO_3$ weight percentages of SN are maximal (50%) in the interglacials except during the ghost sapropel and low in the glacial and the ghost sapropel (minimal 36%) with values fluctuating between 36–44% during MIS100 (Fig. 3d). Total organic carbon weight percentages (not shown) are 0.6% in the ghost sapropel and ~0.16% in the remaining part of the record. Maximum colour reflectance (550 nm) values (36%) at Site 967 are reached at the beginning of MIS101, minimum values (20%) during the ghost sapropel and MIS100 and intermediate values (28–24%) in the rest of the interval.

The $CaCO_3$ of San Nicola and the colour reflectance of Site 967 show an overall similar pattern during MIS101-99. Correlation during MIS100 is modest ($r=0.36$, Table 1) as we abstained from inserting additional age control points within MIS100. It was shown, that the colour reflectance of Site 967 is associated with the calcium carbonate content of the bulk sediment (Wehausen and Brumsack, 1999) so that dark intervals (MIS100 and ghost sapropel) correlate with low carbonate percentages and light intervals (interglacials) with high carbonate percentages. This indicates that sedimentary calcium carbonate content varied with a similar pattern at both Sites during MIS100.

3.3. Planktonic foraminifers

The interglacial stages 101 and 99 are characterised by high percentages of *G. ruber*, *Globorotalia puncticulata*, *Globigerinoides obliquus* and *Globorotalia crassaformis* (Fig. 4). All these species are indicative of warm water and oligotrophic conditions (Bé and Hutson, 1977; Hemleben et al., 1989; Hilbrecht, 1996) with the exception of *G. puncticulata*, which is assumed to be a mixed layer species that profilerates in temperate regions during winter similar to its living relative *Globorotalia inflata* (Bé and Hutson, 1977; Rohling et al., 2004). However, the occurrence of *G. puncticulata* in association with the warm water species *G. ruber* and *G. obliquus* suggests that *G. puncticulata* throve under slightly higher temperatures than modern *G. inflata* as suggested by Kennett and Srinivasan (1983) and Loubere and Moss (1986).

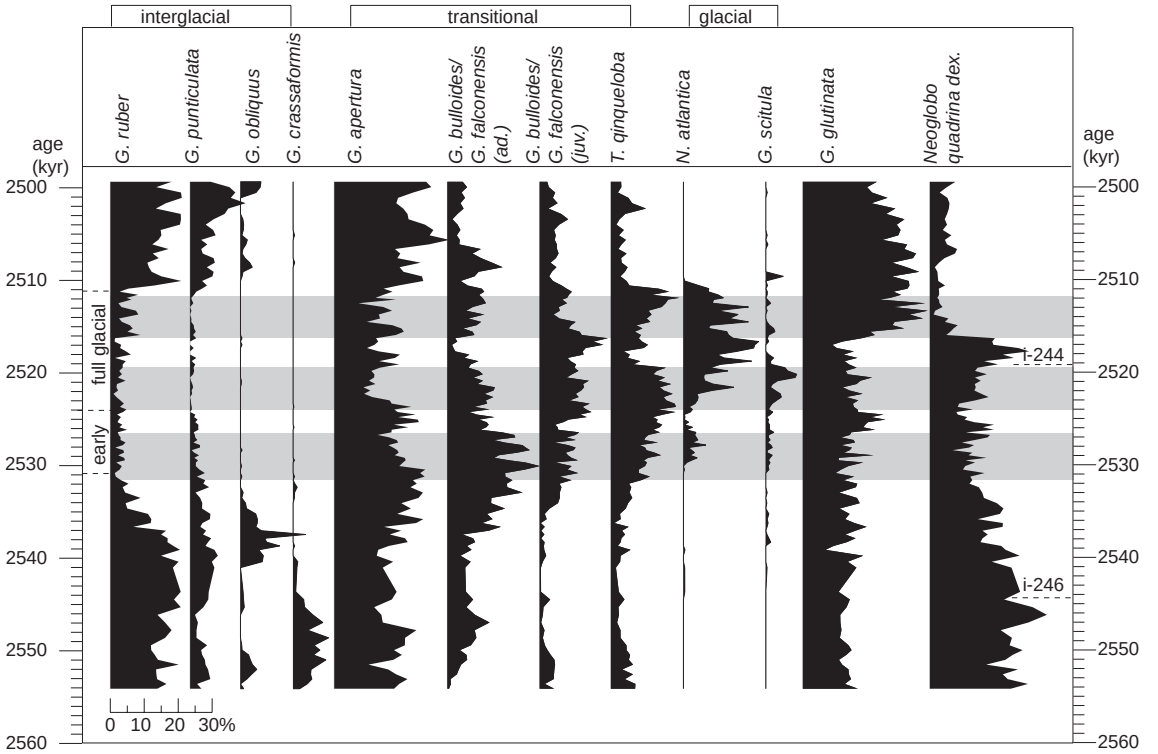

Fig. 4. Relative abundance of the most important planktonic foraminiferal species in the San Nicola MIS100 record versus age. The three different assemblages are indicated on top of the figure. Glacial intervals are marked on the right age-axis.

The warm water species are almost totally absent during the glacial. MIS100 is characterised by the occurrence of *Globorotalia scitula* and *Neogloboquadrina atlantica* with maximum relative abundance being 8% and 29%, respectively, during the full glacial. *G. scitula* and *N. atlantica* are generally associated with cool water (Bé and Hutson, 1977; Hemleben et al., 1989; Zachariasse et al., 1990). *G. scitula* is wide-spread in the Mediterranean throughout the Plio–Pleistocene during glacial times (Zachariasse et al., 1990; Lourens et al., 1992; Rohling et al., 1993). *N. atlantica* is an extinct species that is endemic to high latitudes in Late Miocene to Pliocene times (Poore and Berggren, 1975; Meggers and Baumann, 1997). Morphological studies and biometric measurements indicate that the test size of *N. atlantica* decreased with the Late Neogene global temperature decline (Meggers and Baumann, 1997). Typical sinistrally-coiled *N. atlantica* invaded the Mediterranean first during MIS110 (Lourens et al., 1996) and successively during the following glacial periods associated with MIS108 to MIS96 (Zachariasse et al., 1990) after which it became extinct. Since the appearance of *N. atlantica* is exclusively related to glacial periods this species is clearly associated with surface water cooling in the Pliocene Mediterranean (Zachariasse et al., 1990).

The transition between the interglacial and glacial fauna assemblages is marked by high relative abundances (30%) of *Globoturborotalita apertura*, *G. bulloides/falconensis* and *Turborotalita quinqueloba*. These latter two species are cool water species that proliferate in the Mediterranean winter mixed layer (Rohling et al., 1993, 2004). *G. apertura* probably occurred in warm to temperate waters similar to its living successor *G. rubescens*. *G. apertura* dominates the Mediterranean faunal assemblage of the Early–Late Pliocene but becomes less important towards the end of the Pliocene (Lourens et al., 1992). Lourens et al. (1992) inferred a similar habitat as *G. ruber* but a presumably larger temperature tolerance for *G. apertura* might be suggested from the slightly different

abundance pattern during MIS100. The relative increase in the temperate to cool water species indicates a gradual cooling of the sea surface layer across the glacial boundaries.

The distribution pattern of *Neogloboquadrina* sp. (dex) and *Globigerinita glutinata* seems not related to the glacial–interglacial variability. The distribution of these species shows opposite patterns in accordance with similar observations at the nearby Singa section (Calabria, Italy) for the Late Pliocene time interval (Lourens et al., 1992). Relative abundance of *G. glutinata* is around 15% in the interglacial and the Early and Middle Glacial and rises to 30% at the MIS100.2/MIS100.3 transition. Vice versa, relative abundance of *N.* sp. (dex) is around 30% in the interglacial and Early to Middle Glacial and decreases to 15% at the MIS100.2/MIS100.3 transition. *G. glutinata* lives in the upper 200 m of the Mediterranean water column and is probably more prolific during spring (Rohling et al., 2004). Compared to other species *G. glutinata* has a different feeding strategy as it feeds mainly on diatoms associated with a later stage in productivity blooms (Hemleben et al., 1989; Hilbrecht, 1996). In the Atlantic, high abundance of *G. glutinata* is related to the entrainment of nutrients into the deeper layers by storms (Schiebel et al., 2001). *N.* sp. (dex) is observed to be abundant in deep chlorophyll maxima (DCM) and, therefore, is assumed to proliferate under high-productivity surface water masses and/or stratified surface water conditions (Thunell and Williams, 1989). In the Mediterranean high abundance of *N.* sp. (dex) is often associated with sapropel layers (Rohling and Gieskes, 1989) and with high abundance of *G. ruber*, indicating intensive surface water stratification during relatively warm summers and a seasonal DCM (Lourens et al., 1992; Negri et al., 1999).

We applied a standardised principle component analysis (PCA; SPSS standard software) to further unravel the observed changes in the planktonic foraminiferal abundance patterns. The first two components (PCA-$1_{plankton}$ and PCA-$2_{plankton}$, respectively) explain ~52% of the total variance in the plankton foraminiferal data. Positive scores are recorded for the glacial interval and are related to the cold-water assemblage, including the species *T. quinqueloba*, *G. bulloides/falconensis* (juv), *N. atlantica* and *G. scitula*, whereas negative scores are linked to the warm-water and oligotrophic assemblage, consisting of *G. ruber*, *G. puncticulata*, *G. obliquus* and *G. apertura*. PCA-$1_{plankton}$ is, therefore, interpreted to reflect primarily glacial–interglacial changes in *annual* sea surface temperature (SST_{annual}). This interpretation is strengthened by the good correlation ($r=-0.86$) between PCA-$1_{plankton}$ and $\delta^{18}O_{benthos}$, which both depict the glacial–interglacial transitions as well as the characteristic sawtooth pattern simultaneously (Fig. 5; Table 2). Also on sub-Milankovitch scales PCA-$1_{plankton}$ strongly co-varies with the $\delta^{18}O_{benthos}$ record as evidenced by concomitant changes associated with the sub-stages of MIS100 and the millennial-scale changes within the sub-stages. These shorter events correlate with rapid changes in the abundance of *N. atlantica* (notice the high degree of correlation ($r=0.89$) between *N. atlantica* and $PCA1_{plankton}$). One marked exception is observed during MIS100.3 during which the relative warm SST conditions are interrupted by a short cooling event that corresponds with the most depleted $\delta^{18}O_{benthos}$ values within MIS100 (shaded interval in Fig. 5).

PCA-$2_{plankton}$ is almost exclusively based on the distribution of dextral-coiled *N.* sp. (dex) (positive loadings) versus *G. glutinata* (negative loadings). This component seems to be closely related to the first principal component derived from the total faunal counts of the Singa section (Lourens et al., 1992), which has been interpreted as reflecting primarily changes in sea surface productivity (SSP) conditions. In addition, the trend in PCA-$2_{plankton}$ (Fig. 6) probably reflects the relative decrease in *N.* sp. (dex) associated with the 400-kyr eccentricity minimum between the A and B-sapropel cluster (Lourens et al., 1992). Maximum PCA-$2_{plankton}$ values are observed during i-246 and i-244 (Fig. 6).

3.4. Benthic foraminifers

The glacial–interglacial variability as reflected in the benthic foraminiferal $\delta^{18}O$ is less clear in the benthic composition. In contrast, variation at precessional frequency is clearly visible in the benthic associations and partly interferes with the glacial–interglacial signal. We performed a standardised principal component analysis (PCA; SPSS standard software). For this we reduced the data set by omitting single occurrences, ill-defined taxonomic groups and taxa with relative abundance <1.5%. Unrotated factor scores are plotted in Fig. 5.

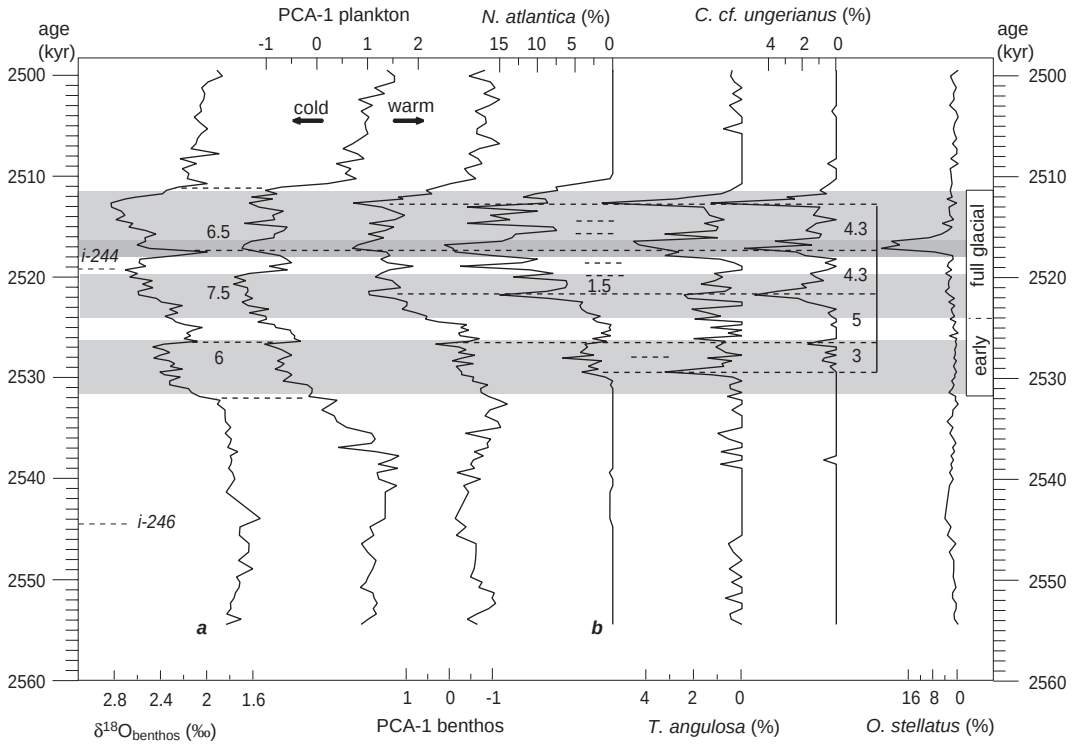

Fig. 5. a) San Nicola $\delta^{18}O_{benthos}$, $\delta^{18}O_{plankton}$, and $PCA1_{plankton}$ and $PCA1_{benthos}$ (inverse x-axis). b) Relative abundance of *Neogloboquadrina atlantica*, *Trifarina angulosa*, *Cibicides* cf. *ungerianus*, *Oridordalis stellatus*. Notice that fauna abundances are plotted on inverse x-axes in order to match with maximum $\delta^{18}O_{benthos}$ (low temperatures). Labelling according to Fig. 3.

The first principal component ($PCA\text{-}1_{benthos}$) explains 18% of the total variance in the data set. Positive scores on the first component are recorded for the full glacial and are related to the relative abundance of *Cibicidoides kullenbergi*, *Globocassidulina subglobosa, Cibicides* cf. *ungerianus*, *Trifarina angulosa*, *Bolivina pseudoplicata* and *Globobulimina* spp (factor loading > 0.6) in association with *Gyroidina orbicularis* and *Oridorsalis stellatus* (factor loading > 0.5). These taxa have a more or less cosmopolitan distribution but some are more commonly associated with relatively cool waters. *T. angulosa*) has been used as an indicator for cold bottom waters in the Pliocene Mediterranean (Zachariasse et al., 1990) and is indigenous to North Atlantic high latitudes in Miocene to recent time (Mackensen et al., 1985; Qvale, 1986). It predominantly occurs in outer shelf to upper slope, well-oxygenated environments (Murray, 1991; Mackensen et al., 1995; Harloff and Mackensen, 1997). Hayward et al. (2002) and Murray (1991) further proposed a relation of *T. angulosa* with low temperatures. *C. kullenbergi* is commonly reported as a surface dweller and associated with

Table 2
Correlation coefficients between selected parameters of SN and Site 967

r	PCA-1 benthos	PCA-1 plankton	*N. atlantica*	*C. kullenbergi*
Site 967	0.56	−0.74	0.61	0.57
$\delta^{18}O_{G.ruber}$	$(0.65)_1$	(0.42)	(0.67)	(0.55)
Site 967	0.80	−0.85	0.77	0.71
$\delta^{18}O_{benthos}$	(0.85)	(−0.69)	(0.70)	(0.69)
SN	0.60	−0.80	0.62	0.59
$\delta^{18}O_{G.ruber}$	(0.63)	(−0.52)	(0.59)	(0.48)
SN	0.76	−0.86	0.76	0.70
$\delta^{18}O_{benthos}$	(0.76)	(−0.61)	(0.66)	(0.64)
PCA1		−0.77	0.89	0.80
Benthos		(−0.76)	(0.83)	(0.83)
PCA1			−0.74	−0.67
Plankton			(−0.52)	(−0.47)

1) Numbers in brackets are coefficients for MIS100 only.

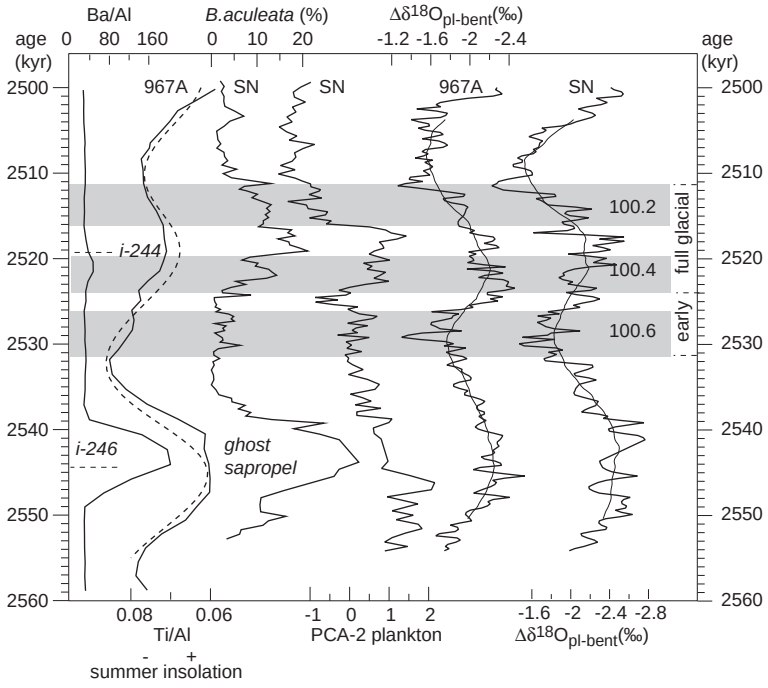

Fig. 6. ODP Site 967A $\Delta\delta^{18}O_{plankton–benthos}$ (overlain by moving average), San Nicola $\Delta\delta^{18}O_{plankton–benthos}$ (overlain by moving average) and $PCA2_{plankton}$ in relation to ODP Site 967A Ba/Al, Ti/Al (inverse axis) and $Laskar04_{(1,1)}$ 65°N summer insolation. Labelling according to Fig. 3.

well-aerated bottom waters and low organic flux (Lutze and Colbourn, 1984; Corliss, 1985; Fariduddin and Loubere, 1997; Schmiedl et al., 1997). Its recent distribution appears to be associated with cooler water-masses off West Africa (Lutze and Colbourn, 1984) and Schmiedl et al. (1997) stress its co-occurrence with North Atlantic Deep Water (NADW). From a perspective of trophic and oxygenation state of bottom waters, the behaviour of *Trifarina angulosa* and *Bolivina pseudoplicata* is quoted by Verhallen (1991) as intermediate between opportunistic and equilibrium. For *T. angulosa* a relation with high (Gupta, 1997; Harloff and Mackensen, 1997) as well as with low organic flux rates (Mackensen et al., 1995) is documented. *G. orbicularis* is mentioned as an opportunistic taxon requiring ventilated bottom waters (Jorissen et al., 1992). Ecological preferences of *Oridorsalis* spp. are under debate. *O. umbonatus* is considered an opportunistic taxon, related to elevated organic flux by (1995), Miao and Thunell (1996) and Kuhnt et al. (1999). At similar latitudes it is found to be abundant in the glacial as well as in the interglacial (Jian et al., 1999).

Negative scores on the $PCA\text{-}1_{benthos}$ are related to the relative abundances of costate buliminids, *Bolivina spathulata*, *Uvigerina peregrina* and *Siphonina recticulata*. The first three species are indicative for slightly depleted bottom water oxygenation and relatively high and continuous organic matter supply (Verhallen, 1991; Schmiedl et al., 2003). Rathburn and Corliss (1994) report *Siphonina* from thermospheric (>10 °C) waters in the Sulu Sea. Positive $PCA\text{-}1_{benthos}$ scores are interpreted to represent well-ventilated, possibly cooler bottom waters during the full glacial with an intermittent organic matter supply to the sea floor.

The distribution pattern of the non-costate buliminids is related to precessional cyclicity. These taxa abound during precession minima i-246 (the ghost-sapropel) and to a lesser extent i-244 (Fig. 6). Non-costate buliminids are mentioned in relation to fine-grained substrates and elevated productivity and/or lowered bottom-water oxygenation (Mackensen et al., 1993; Fariduddin and Loubere, 1997; Gupta, 1997; Jannink et al., 1998; Jian et al., 1999; Hayward et al., 2002).

4. Discussion

4.1. Milankovitch-scale climate variability

4.1.1. Sea surface temperatures

The $\delta^{18}O_{benthos}$ glacial–interglacial differences at San Nicola and Site 967 are in good agreement with open ocean benthic isotope records (Raymo et al., 1989; Shackleton et al., 1995) and are, therefore, interpreted to represent dominantly obliquity-controlled variations in global ice volume. The ice volume effect during MIS100 was estimated to be ~0.8‰ (Raymo et al., 1989, 1992), which is in agreement with the rapid deglaciation in our Mediterranean $\delta^{18}O_{benthos}$ records at the MIS100/99 transition and leaves only a minor temperature and/or salinity-related component for the Mediterranean $\delta^{18}O_{benthos}$ records of ~0.2‰. Modelling experiments suggest that the evaporation/precipitation (E–P) balance did not change significantly during glacial times (Bigg, 1995), therefore excluding a significant salinity effect on the $\delta^{18}O_{benthos}$ record. However, it remains uncertain to infer regional $\delta^{18}O_{sw}$ (sw: sea water) from a purely E–P basis, because on a local scale the degree of mixing in intermediate waters to a few hundred metres below the sea surface may alter the $\delta^{18}O_{sw}$ significantly (Bigg, 1995). Additionally, the $\delta^{18}O$ measured on specific foraminifera species might be biased towards a very specific growth season or optimum temperature at which the species calcify. Furthermore, the $\delta^{18}O_{sw}$ of the inflowing Atlantic surface water and sea level-related difference in the sill depth of Gibraltar and Sicily may have influenced the $\delta^{18}O_{sw}$ of the Mediterranean even if the E–P balance remained similar. The good correlation between the $\delta^{18}O_{benthos}$ and PCA-$1_{plankton}$ may indicate that at least part of the (glacial-bound) reduced SST_{annual} conditions at glacial times has been exported towards deeper waters. Based on the empirical temperature–$\delta^{18}O$ relationship of 1 °C/0.25‰ (Shackleton, 1967; O'Neil et al., 1969), the MIS100-bound temperature decrease should have been less than 1 °C for the deeper waters.

The $\delta^{18}O_{G.ruber}$ glacial–interglacial amplitude is larger (by ~0.4‰ at San Nicola and 0.1‰ at Site 967) than that of the $\delta^{18}O_{benthos}$ and indicates that planktonic $\delta^{18}O$ records are additionally affected by small changes in temperature and/or salinity. Preliminary $U^{K'}_{37}$ data indicate that average SST_{annual} at San Nicola was ~6°C lower during MIS100 than during the adjacent interglacial stages (Menzel pers. comm., 2004). This is in agreement with SST reconstruction from the last glacial maximum (LGM) in the western and eastern Mediterranean Sea (Kallel et al., 1997b; Cacho et al., 1999; Paterne et al., 1999) but disagrees with the observed $\delta^{18}O_{G.ruber}$ glacial–interglacial amplitude during MIS100. However, the $\Delta T_{glacial-interglacial}$ component of the $\delta^{18}O_{G.ruber}$ might be underestimated because *G. ruber* is known to calcify at optimum temperatures during the summer season (Schmidt and Mulitza, 2002). This could have biased the oxygen isotope signal towards warmer SST, since only the warmest summers are recorded by *G. ruber* and colder summers are 'skipped'. As a result the δT_{annual} should have probably been larger, implying that the δT_{annual} recorded by the alkenones is not necessarily larger than the δT_{summer} recorded by *G. ruber*.

We subtracted the $\delta^{18}O_{benthos}$ values of Site 967 from both $\delta^{18}O_{G.ruber}$ records to reconstruct this additional (combined temperature and salinity) effect. For this purpose all $\delta^{18}O$ records were interpolated at 250-year steps. We used the $\delta^{18}O_{benthos}$ of site 967 as reference because this site is deeper and, therefore, assumed to reflect ice volume changes more appropriate. Remarkably, the resulting $\Delta\delta^{18}O_{G.ruber-benthos}$ records of both San Nicola and Site 967 closely follow the precession-dominated summer insolation pattern and much less the obliquity-controlled PCA-$1_{plankton}$ and SST (Fig. 6). It appears that the amplified $\delta^{18}O_{G.ruber}$ values are not controlled by the glacial–interglacial SST_{annual} variability, but reflect merely the influence of precession-bound surface water salinity (SSS) and/or SST changes. Evidently, periods of maximum absolute $\Delta\delta^{18}O_{G.ruber-benthos}$ values correspond with the summer insolation maxima i-244 and i-246 reflecting a more stratified water column at times of high seasonality.

The fact that precession exerts the main control on eastern Mediterranean climate and hydrography during the Plio–Pleistocene has been extensively shown by studies on Mediterranean marine cores and land-based marine successions (Lourens et al., 1992; Hilgen, 1991a; Hilgen et al., 1993, 1995). Microfossil assemblages, pollen and stable isotope data have indicated that the principal climate variability in the pre-

cession frequency band is related to changes in warm–wet and cold–dry conditions (Cita et al., 1977; Vergnaud-Grazzini et al., 1977; Rossignol-Strick, 1983; Kallel et al., 1997a, 2000). The most characteristic sedimentary expression of the precession-controlled climate variability is the regular and cyclic occurrence of sapropels, which has often been associated with changes in river-runoff and circum-Mediterranean humidity (Rohling and Hilgen, 1991). These conditions are generally linked to an intensified African monsoon circulation causing a low salinity surface water lens in the eastern Mediterranean and hence stagnant bottom waters during minimum precession (Rossignol-Strick, 1983, 1985). The existence of a low salinity surface water lens is evidenced by very depleted $\delta^{18}O_{plankton}$ values of in particular *G. ruber* (Vergnaud-Grazzini et al., 1977; Rossignol-Strick et al., 1982; Kallel et al., 1997a; Emeis et al., 2003; Rohling et al., 2004). Such a low salinity lens may in turn have induced a shoaling of the pycnocline into the nutricline and resulted in the development of a deep chlorophyll maximum (DCM) (Rohling and Hilgen, 1991).

In the interval of MIS101-99 no sapropels are deposited at San Nicola and Site 967, but the existence of a ghost sapropel and the minima in Ti/Al (Lourens et al., 2001) and maxima in absolute $\Delta\delta^{18}O_{G.ruber–benthos}$ during summer insolation maxima i-244 and i-246 indicate that climate conditions were not much different from those leading to sapropel formation. The elevated Ba/Al contents at ODP Site 967 (Wehausen and Brumsack, 1999) and the high PCA-$2_{plankton}$ values at San Nicola furthermore point to enhanced primary productivity during i-244 and i-246 possibly as a result of a distinct (seasonal) DCM. Such an increase in SSP conditions may have increased the oxygen consumption rate in the bottom water as indicated by the relative abundance of noncostate buliminids in the benthic foraminiferal assemblages (Fig. 6).

4.1.2. Response times

The obliquity-forced SST and $\delta^{18}O_{benthos}$ are in phase with one another and lag obliquity by ~8 kyr (Figs. 3 and 5). This estimate is in very good agreement with the outcome of simple ice sheet models applied to explain the Late Pleistocene glacial cyclicity (Imbrie and Imbrie, 1980; Imbrie et al., 1984). A similar time lag was applied for the construction of astronomical time scales based on tuning open ocean benthic isotope records of Pliocene and Early Pleistocene age to the obliquity time series (Raymo et al., 1989; Ruddiman et al., 1989; Shackleton et al., 1990). The obliquity-related time lag, however, may have been variable through time because of changes in the response time of the climate system related to the size of the ice sheets (Oerlemans and van der Veen, 1984). A reduced ice sheet during the Pliocene would result in a smaller time constant and a reduction of the obliquity lag (Chen et al., 1995). Despite the different size in ice sheet and the different duration of the glacials in Late Pliocene compared to Late Pleistocene, the behaviour of the ice sheet to obliquity forcing was probably the same. The saw-tooth structure of the San Nicola and Site 967 $\delta^{18}O_{benthos}$ records confirms the asymmetric ice sheet development (slow growing and fast waning) predicted in models for Late Pleistocene ice sheet behaviour (Imbrie et al., 1984; MacAyeal, 1993).

Small uncertainties in the astronomical solution and in the adopted precession-related response time of the climate system may significantly alter the outcome of the obliquity-related lag (Lourens et al., 1996; 2001). However, for the investigated time interval the theoretical changes in tidal dissipation and dynamical ellipticity will change the obliquity-related time lag one kyr at most (Lourens et al., 2001). More important is the uncertainty in the response time of the climate system to precession forcing. In our age model the time lag with respect to precession forcing was set to zero assuming an immediate response of Ti/Al to African aridity changes. This assumption differs from that of Lourens et al. (1996) who incorporated a time lag of 3 kyr based on the age difference between the AMS ^{14}C-dated midpoint of the youngest Holocene sapropel, S1 (~8.5 ka), and the correlative summer insolation maximum at 11.5 ka. Lourens et al. (1996) suggested that this lag could be related to the modelled ~3 kyr time lag of the maximum summer temperature (T_{max}) in northern Africa with respect to the precession parameter (Short and Mengel, 1986) applying an Energy Balance Model. Short and Mengel (1986) argued that T_{max} may be an indication of the moisture availability to the monsoon area during the rainy season, which could therefore explain the observed lag between a monsoon trigger

of sapropel formation and precession. Recently Tuenter et al. (2005) carried out transient runs with an intermediate complexity climate model (CLIMBER2.3) to test the scenario of Short and Mengel (1986). These experiments revealed that T_{max} at low-latitudes (15°N) indeed lags the precession parameter, but that no time lag was observed between the African–Indian monsoon annual precipitation and the precession parameter. This implies that either sapropel formation in the Mediterranean is not (only) linked to changes in African–Indian monsoon annual precipitation but probably influenced by the Atlantic system or that the time lag estimate of the S1 is an exception. The latter option however seems unlikely because the timing based on ^{230}Th–U (TIMS) of peak hydrological conditions associated with sapropels S1–S5 as evidenced from speleothems (Soreq cave, Israel) also points to a significant lag of 3–5 kyr (Bar-Matthews et al., 2000). This estimate clearly falls in the range of the lag adopted by Lourens et al. (1996) and the 5-kyr time lag modelled for the precession-bound ice sheet response time of the Late Pleistocene glacial cycles (Imbrie and Imbrie, 1980; Imbrie et al., 1984). Presumably, the slow changes in ice volume may have an effect on the time lag between precession and the peak humid climate conditions associated with sapropel midpoints of the Late Pleistocene. Application of a 3–5 kyr lag instead of the zero lag used in the present study will increase the obliquity-related time lag to ~11–13 kyr for MIS100. This large lag cannot be simply explained in terms of ice sheet dynamics and is, therefore, highly unlikely. Moreover, the role of precession-related high-latitude variability in global ice volume during the Late Pliocene to Early Pleistocene is not evident (Raymo et al., 1989; Ruddiman et al., 1989). All this suggests that during the Late Pliocene the response time for the precession-related dry–wet oscillations of circum-Mediterranean climate are most likely in phase with the precessional forcing and, hence, could be primarily driven by changes in the intensity of the African–Indian monsoon.

4.2. Sub-Milankovitch scale climate variability

4.2.1. Changes on a stadial–interstadial time scale

The registration of sub-Milankovitch scale climate variability is most evident from the rapid decreases in the $\delta^{18}O_{benthos}$ of San Nicola and concomitant SST_{annual} changes associated with the sub-stages of MIS100. Episodes of relatively warmer SST conditions interrupt the overall colder glacial conditions and coincide with interstadials MIS100.3 and MIS100.5. Each of these warm phases is preceded by a gradual cooling trend during the stadials MIS100.2, MIS100.4, and MIS100.6. The sawtooth pattern in combination with the average duration of ~6–8 kyr shows strong similarities with the so-called Bond-cycles during the Late Pleistocene (Bond, 1992; Bond et al., 1993; Bond and Lotti, 1995) and hence may indicate a direct coupling between North Atlantic and Mediterranean high-frequency climate changes. This interpretation is confirmed by North Atlantic sedimentary records, which indicate ice rafting events during MIS100 that have a similar temporal spacing (5–7 kyr) as the San Nicola $\delta^{18}O_{benthos}$ and SST_{annual} sub-stages (Becker et al., in press).

The remarkable absence of distinct sub-Milankovitch scale cycles in the $\delta^{18}O_{benthos}$ of Site 967 indicates that the inferred climate changes were most likely not accompanied by significant changes in global ice volume. Moreover, amplitudes of sub-cycle changes in the San Nicola $\delta^{18}O_{benthos}$ record are of almost the same magnitude as glacial–interglacial variations, which would imply melting of large parts of land-based ice sheets within a few hundred years. Although fast waning of ice-sheets is in accordance with current ice sheet models, ice sheet growth requires more time (MacAyeal, 1993) than the San Nicola benthic oxygen isotope record indicates. This is illustrated at the beginning of MIS100 where San Nicola $\delta^{18}O_{benthos}$ increases by 0.4‰ within 2 kyr, while it takes ~6 kyr to reach the same change in the $\delta^{18}O_{benthos}$ of Site 967 (Fig. 3). An increase of 0.4‰ is half the total ice volume-estimate for MIS100 implying an ice sheet accumulation to half its size within 2 kyr. This is clearly not in agreement with ice sheet models and indicates that the sub-cycles in the San Nicola $\delta^{18}O_{benthos}$ record are most likely caused by other mechanisms. These mechanisms may be directly linked to changes in the properties and volume of the inflowing North Atlantic surface waters and/or indirectly by changes in the intensity and position of atmospheric pressure gradients in the North Atlantic region.

North Atlantic surface waters may show depleted $\delta^{18}O$ values because of the large input of isotopic light melt water as consequence of massive iceberg melting in the North Atlantic. The $\delta^{18}O$ of *Neogloboquadrina pachyderma* during Heinrich event 4 (H4) for example shows a maximum drop of 2‰ right in the centre of maximum iceberg discharge but decreases quickly at greater distances (i.e., off Portugal, amplitudes were much smaller than 0.5‰) (Cortijo et al., 1997). The San Nicola $\delta^{18}O$ records show changes in the order of 0.4–0.8‰ during the sub-stages of MIS100, which require even more extreme iceberg melting events than during H4. It seems, therefore, unlikely that the strong depletion in the San Nicola $\delta^{18}O$ records originate from the inflow of low salinity Atlantic surface water alone.

4.2.2. Changes in Mediterranean thermohaline circulation

The strong similarity of the San Nicola $\delta^{18}O_{benthos}$ sub-stages with the $\delta^{18}O_{G.ruber}$ ($r=0.88$, Table 1) and SST record ($r=-0.86$, Table 1) suggests a coupling to surface water cooling events. In the present-day Mediterranean, deep and intermediate water is formed above all during boreal winter, when latent heat loss and surface cooling are strongest and initiate thermocline deepening and, subsequently, deep mixing (Pinardi and Masetti, 2000). Temperature of the surface water during winter, therefore, determines the temperature of deep and intermediate water and, hence, influences the oxygen isotope composition of benthic foraminifers.

The peak abundances of *N. atlantica*, *C. cf. ungerianus*, and *T. angulosa* indicate a high-frequency component that is superimposed on the obliquity-controlled ice volume/temperature signal and occurs simultaneously in the surface and deeper waters (Fig. 5). The fast fluctuations in the abundance of *C. cf ungerianus* and *T. angulosa* could also indicate a response to a more pulsating export production and convective overturning regime during MIS100. Although, *N. atlantica* is assumed to be related to temperature, peak abundances in *N. atlantica* could also be related to productivity-related nutrient pumping from a seasonal DCM. However, little is known about the feeding strategy of *N. atlantica*. As *N. atlantica* is probably ancestral to the modern *Neogloboquadrinids* it could have had a similar feeding strategy as *Neogloboquadrina* relying on high phytoplankton productivity. At San Nicola highest relative abundances in *N. atlantica* are accompanied by high abundances of *Neogloboquadrina* with exception of MIS100.4 (Fig. 4). In any case, the concomitant peak abundances of these species may indicate that winter cooling and deep mixing were at a maximum. Such a scenario would be in analogy with Late Pleistocene peak abundances of left-coiling *N. pachyderma* found in cores from the Gulf of Lions during Heinrich events (Rohling et al., 1998). Within MIS100, the severe winter cooling conditions coincide with the stadial phases and with interstadial MIS100.3. The latter exception closely matches with the interval of strongly depleted $\delta^{18}O_{benthos}$ values associated with MIS100.3 at San Nicola. At Site 967, this interval is characterised by heavy $\delta^{18}O_{benthos}$ values, which approximate the values recorded during the last phase of MIS100.4, which may point to full glacial conditions as well. Despite this uncertainty, it is obvious that the strong winter cooling events take place during the most extreme glacial conditions of MIS100. These events occur rather regularly with average spacing of ~1.5–4.5 kyr (Fig. 5), which is similar to the spacing of variations found in the Late Pleistocene oxygen isotope and $U_{37}^{K'}$ records of the western Mediterranean Sea (Cacho et al., 2000, 2002). These events have been unambiguously correlated to the Dansgaard–Oeschger cycles and Heinrich events in the Greenland ice cores and North Atlantic sediments. Cacho and co-workers argued that the variability in the oxygen isotope and $U_{37}^{K'}$ records of the western Mediterranean Sea reflects changes in surface water-cooling and deep-water formation as an immediate response to the North Atlantic climate changes. This is partly caused by the direct inflow of cold Atlantic surface waters but most importantly by an indirect atmospheric connection.

Pollen data showed that with the extension of glaciers and sea ice in the Northern Hemisphere, polar air masses expanded southward and cooled the European continent during MIS100 (Willis et al., 1999) and subsequent glacial stages (Combourieu-Nebout, 1991). This southward expansion of polar air masses may have set the stage for more frequent and intense cold air outbreaks over the central Mediterranean (San Nicola) and more frequent Atlantic depressions entering the Mediterra-

nean. To resume, we hypothesize that both cooler Atlantic surface water and cooler and more frequent Atlantic depressions caused intensified surface water-cooling and deep convection during stadial phases MIS100.2, MIS100.4 and MIS100.6. The strength of winter mixing depends, however, not only on winter conditions but also on the internal structure of the water column before winter cooling. A weaker stratification would facilitate winter mixing while summer stratification isolates the deeper water from surface processes (Pinardi and Masetti, 2000). Changes in these water column properties may explain the high frequency alternations of peak occurrences of *N. atlantica* and *G. scitula* (Fig. 4). During interstadial MIS100.5 the intensified winter cooling and deep mixing ceased and the climate state returned to the background MIS101/MIS100 transition as indicated by the intermediate $\delta^{18}O_{benthos}$ values at San Nicola and Site 967 and the drop in *N. atlantica* percentages.

4.2.3. Exceptional interstadial MIS100.3

It seems highly unlikely that the strong depletion in the $\delta^{18}O_{benthos}$ record of San Nicola during interstadial MIS100.3 also reflects more interglacial climate conditions with a generally warmer atmosphere and a weaker wind field preventing severe winter cooling and deep convection. Such a scenario is in particular rejected by the highest abundance of *N. atlantica* within MIS100 and the peak occurrences of *C. cf. ungerianus*, and *T. angulosa*, indicating that winter cooling and deep mixing were at their maximum. Moreover very depleted $\delta^{18}O_{G.ruber}$ values during MIS100.4 and early MIS100.3 in combination with high SSP, low SST_{annual} and low $U_{37}^{K'}$ point towards a low salinity surface layer related to precessional forcing of insolation cycle i-244. A sharp decrease in the $\delta^{18}O_{G.ruber}$ during the middle of MIS100 coincides with the strong depletion in the $\delta^{18}O_{benthos}$ record of San Nicola, indicating the transfer of depleted surface water $\delta^{18}O$ towards deeper waters by intensified winter mixing. A similar mechanism has been proposed for the interruption of the sapropel S1 (de Rijk et al., 1999) and S5 (Rohling et al., 2004). The prominent peak of *O. stellatus* (Fig. 5b) probably confirms this mechanism. *O. stellatus* is an opportunistic benthic foraminifer and among the first taxa to re-colonise the benthic realm after the Messinian salinity crisis (Sprovieri and Hasegawa, 1990) and thought to be tolerant to salinity changes (Seidenkrantz et al., 2000). The development of a low-salinity surface water layer in contrast to severe winter mixing illustrates that different climate mechanisms interfere (a combination of Milankovitch and sub-Milankovitch related processes) making MIS100.3 an exceptional interval.

The absence of MIS100.3 and to a lesser extent MIS100.5 in the $\delta^{18}O_{benthos}$ of Site 967 suggests that the eastern Mediterranean was not sensitive to winter mixing during MIS100 or that deeper waters at Site 967 were not coupled to surface water. Similar to the western Mediterranean, present-day deep-water formation in the eastern Mediterranean basin is related to winter surface cooling by cold air outbreaks from the European continent and subsequent vertical convection. Additional mixing with high saline intermediate water results in a cold saline deep water mass (Pinardi and Masetti, 2000). If deep-water circulation during MIS100 was similar to today either winter cooling in the eastern Mediterranean was not efficient or intermediate-water not saline enough. From the $\delta^{18}O_{G.ruber}$ it can be argued that surface waters at Site 967 were significantly different from the central Mediterranean during MIS100 and were probably not affected by the North Atlantic pressure system on sub-Milankovitch time-scales.

4.3. High latitude versus low latitude climate variability

Evidence for concomitant high-frequency climate variability in the eastern and western Mediterranean comes from sedimentary colour reflectance and magnetic susceptibility data of different ODP Leg 160 and 161 sites (Shipboard data, ODP Leg 160 and 161 data bases). Variations in calcium carbonate and colour reflectance also co-occur in San Nicola and Site 967 (Fig. 3d) and to a higher degree in San Nicola and ODP Site 969D (Fig. 7, for location of Site 969 see Fig. 1) reflecting basin-wide changes in the bulk composition of the sediment. Although the mechanisms behind these changes are not fully understood, these changes are primarily driven by (i) carbonate productivity, (ii) dilution of carbonates by aluminosilicates or (iii) dissolution of carbonates with (i) and (ii) being the most important factors for Pliocene

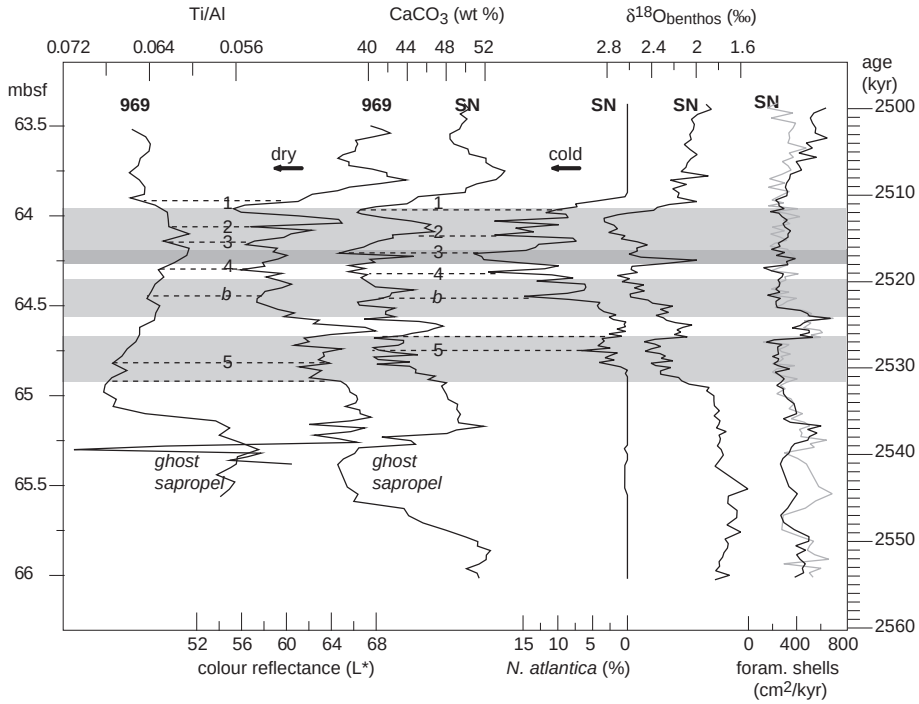

Fig. 7. ODP Site 969D Ti/Al (data of Wehausen, 1999) and colour reflectance (L*) versus depth (mbsf). Horizontal stippled lines and labels indicate intervals with high Ti/Al and low colour reflectance values. Site 967 $CaCO_3$, N. atlantica, $\delta^{18}O_{benthos}$ and planktonic (black line) and benthic (grey line; benthic fluxes are multiplied by a factor 10 to match with *x*-axis) foraminiferal fluxes versus age. Notice inversed *x*-axes for $CaCO_3$, *N. atlantica* and $\delta^{18}O_{benthos}$. Horizontal stipple lines and labels indicate intervals with low $CaCO_3$ and cold Dansgaard–Oeschger phases. Further labelling according to Fig. 3.

carbonate cycles on Sicily (van Os et al., 1994) and for ODP Site 967 and Site 969 (Wehausen, 1999). Low carbonate productivity during MIS100 is evidenced by low foraminiferal fluxes at San Nicola but variability in these fluxes is too small to explain the observed changes in the sediment properties except for interstadial MIS100.5 (Fig. 7). Also changes in the fluxes of calcareous nannoplankton would be unlikely to be large enough to cause these changes in $CaCO_3$, so that dilution of carbonates by aluminosilicates during times of lowered carbonate productivity seems to be the most important mechanism with either wind-blown or fluvial transported material as major aluminosilicate source. A synchronous basin-wide variation in terrestrial sediment supply would favour wind-blown rather than fluvial transported material.

The most important dust source for the present day Mediterranean is the African continent, especially the Sahara and its peripheral regions (Guerzoni and Roy, 1996). Although dust is exported to the Mediterranean all year round, major dust storms across the Mediterranean occur during spring and summer, when atmospheric depression systems lie over the Saharan region (Dulac et al., 1996). Deposition of Saharan dust in the Mediterranean is estimated to several million tons $km^{-2}\,y^{-1}$ with a strong year-to-year variability (Prospero, 1996) being sensitive to even minor changes in the source region climate and the dust transport path. Particularly changes in the atmospheric vertical stability and the precipitation regime affect the rate at which dust is lifted and deposited and changes in the storm tracks can modify the seasonality of dust storm events (Giorgi, 1996).

Clay mineral analyses and geochemical data of Mediterranean sediments indicate an increase in the relative contribution of Sahara dust during insolation minima, which is commonly interpreted to be linked to low African monsoon activity and drought in North Africa during precession maxima (Foucault

and Mélières, 1995; Wehausen and Brumsack, 1999; Foucault and Mélières, 2000; Lourens et al., 2001). As indicated by the Ti/Al record of Site 967, dust supply during MIS99-101 was similarly related to African aridity and strength of Saharan depressions and varied in phase with summer insolation. However, short-term fluctuations are evident in the Ti/Al of Site 969D (data Wehausen (1999)) (Fig. 7). High Ti/Al values correlate with dark sediments and thus low $CaCO_3$ values indicating peak dust episodes during intervals with low $CaCO_3$. Comparison with the $CaCO_3$, *N.atlantica* and $\delta^{18}O_{benthos}$ record of San Nicola indicates further that these dust episodes during MIS100 are contemporaneous with vigorous surface water cooling and deep convection in the central Mediterranean during the cold intervals of the D–O cycles (Fig. 7).

Such a relationship has been observed in the Mediterranean paleoclimate record of the past 50 kyr (Allen et al., 1999; Moreno et al., 2001; Combourieu-Nebout et al., 2002; Sanchez-Goni et al., 2002; Moreno et al., 2004). These studies attribute dry phases with increased dust transport from the Sahara to the western and central Mediterranean to a strengthening and a northward displacement of the North-Westerlies during stadial intervals similar to present day high NAO (North Atlantic Oscillation) index years. During theses times, prolonged winter anticyclones stability over central and northern Europe may have resulted in a strong flow over the Mediterranean region and very cold and dry Mediterranean winters and may have favoured the dryness in Mediterranean during stadial phases in addition to a more vigorous atmospheric circulation over the western and central Mediterranean region.

Although this interpretation renders no explanation for the difference in seasonality and the exact phasing of spring/summer dust plumes and winter water column instability it is in agreement with general circulation models that suggest that Atlantic SST could influence African climate by strengthening the subtropical pressure cell and effecting both dust source area aridity and intensity of the dust transporting trades (deMenocal and Rind, 1993). During minimum eccentricity forcing and thus minimum insolation amplitude, the African continent would be most sensitive for high latitude forcing (deMenocal and Rind, 1993).

5. Conclusions

Obliquity related changes in SST and global ice volume at San Nicola and Site 967 during MIS101-99 are in phase with one another and lag obliquity by ~8 kyr. This time lag is in agreement with open ocean Pleistocene records and ice sheet models. Precession-related variability is evident in the fauna and oxygen isotope data indicating that dry–wet oscillations within MIS100 were not so much different from the climate changes linked to sapropel formation. These dry–wet oscillations are in phase with precession and most likely driven by changes in the African–Indian monsoon although the simultaneous influence from the Atlantic system may have played a role (Tuenter et al., 2005).

The absence of sapropels in San Nicola and ODP Site 967 and Site 969 during MIS100 indicates a weakened monsoonal circulation related to the 400-kyr eccentricity minimum. Consequently, the atmospheric connection to the North Atlantic pressure system was probably extended allowing Atlantic depressions to enter further into the Mediterranean and more indirectly initiating downwind cooling from the Alps. Therefore, stadial–interstadial climate changes in the western and central Mediterranean are probably directly related to changes in the strength of the North Atlantic atmospheric wind field. Stadial phases are associated with short-time sea surface cooling events causing intensive stirring and deep convection. These cooling events are very similar to the Dansgaard–Oeschger and Heinrich events that occurred during the Late Pleistocene in the western Mediterranean. The absence of such high-frequency climate variations in the eastern Mediterranean suggests that this part of the Mediterranean was either decoupled from or not sensitive to North Atlantic climate forcing.

Episodes of Mediterranean-wide increase in the Sahara dust deposition are evidenced by the sedimentary calcium carbonate of San Nicola and Ti/Al of Site 969D during the cold intervals of the D–O and HE-like events. Although the origin of this high-frequency component is clearly the African continent, the similarity with high latitude climate features suggests a linkage between high and low latitude climate possibly through the North Atlantic pressure system. The data further indicate, that high-frequency climate

change is highly complex in the Mediterranean due to the interference of climate variations forced by the primary Milankovitch frequencies.

Acknowledgements

This research was carried out within the framework of the PIONEER-programme of F.J. Hilgen, which is financially supported by the Netherlands Organization for Scientific Research (NWO), and partly funded by EU Project 'Paleostudies' contract No.: HPRI-CT-2001-0124.

References

Allen, J.R.M., Brandt, U., Brauer, A., Hubberten, H.W., Huntley, B., Keller, J., Kraml, M., Mackensen, A., Mingram, J., Negendank, J.F.W., Nowaczyk, N.R., Oberhansli, H., Watts, W.A., Wulf, S., Zolitschka, B., 1999. Rapid environmental changes in southern Europe during the last glacial period. Nature 400, 740–743.

Bar-Matthews, M., Ayalon, A., Kaufman, A., 2000. Timing and hydrological conditions of Sapropel events in the eastern Mediterranean, as evidenced from speleothems, Soreq cave, Israel. Chem. Geol. 169, 145–156.

Bé, A.W.H., Hutson, W.H., 1977. Ecology of planktonic foraminifera and biogeographic patterns of life and fossil assemblages in the Indian Ocean. Micropaleontology 23, 369–414.

Becker, J., Lourens, L.J., Raymo, M.E., in press. High-frequency climate linkages between the North Atlantic and the Mediterranean during Marine Oxygen Isotope Stage 100 (MIS100). Paleoceanography.

Bigg, G.R., 1995. Aridity of the Mediterranean Sea at the last glacial maximum: a reinterpretation of the $d^{18}O$ record. Paleoceanography 10 (2), 283–290.

Bonaduce, G., Sprovieri, R., 1984. The appearance of *Cyteropteron testudo* Sars (Crustacea: Ostracoda) is a Pliocene event. Evidence from the south-central Mediterranean. Boll. Soc. Paleontol. Ital. 23, 131–136.

Bond, G.C., 1992. Evidence for massive discharges of icebergs into the North Atlantic ocean during the last glacial period. Nature 360, 245–249.

Bond, G.C., Lotti, R., 1995. Iceberg discharges into the North Atlantic on millennial time scales during the last glaciation. Science 267, 1005–1010.

Bond, G.C., Broecker, W., Johnsen, S., McManus, J., Labeyrie, L., Jouzel, J., Bonani, G., 1993. Correlations between climate record from North Atlantic sediments and Greenland ice. Nature 365, 143–147.

Bond, G.C., Showers, W., Elliot, M., Evans, M., Lotti, R., Hadjas, I., Bonani, G., Johnson, S., 1999. The North Atlantic's 1–2 kyr climate rhythm: relation to Heinrich events, Dansgaard/Oescher cycles and the Little Ice Age, mechanisms of global climate change at millennial time scales. Geophys. Monogr., 35–58.

Bond, G.C., Kromer, B., Beer, J., Muscheler, R., Evans, M.N., Showers, W., Hoffmann, S., Lotti-Bond, R., Bonani, G., 2001. Persistent solar influence on North Atlantic climate during the Holocene. Science 294, 2130–2136.

Cacho, I., Grimalt, J.O., Pelejero, C., Canals, M., Sierro, F.J., Flores, J.-A., Shackleton, N.J., 1999. Dansgaard–Oeschger and Heinrich event imprints in Alboran sea paleotemperatures. Paleoceanography 14 (6), 698–705.

Cacho, I., Grimalt, J.O., Sierro, F.J., Shackleton, N., Canals, M., 2000. Evidence for enhanced Mediterranean thermohaline circulation during rapid climatic coolings. Earth Planet. Sci. Lett. 183 (3–4), 417–429.

Cacho, I., Grimalt, J.O., Canals, M., 2002. Response of western Mediterranean Sea to rapid climatic variability during the last 50,000 years: a molecular biomarker approach. J. Mar. Syst. 33–34, 253–272.

Carter, S.J., Raymo, M.E., 1999. Sedimentological and mineralogical control of multisensor track data at Sites 981 and 984. In: Raymo, M.E., Jansen, E., Blum, P., Herbert, T.D. (Eds.), Proceedings of the Ocean Drilling Program, Scientific Results. ODP, College Station, Texas, pp. 247–256.

Chen, J., Farrell, J.W., Murray, D.W., Prell, W.L., 1995. Time scale and paleoceanographic implications of a 3.6 m.y. oxygen isotope record from the north east Indian Ocean (Ocean Drilling Program Site 758). Paleoceanography 10 (1), 21–47.

Cita, M.B., Vergnaud-Grazzini, C., Robert, C., Chamley, H., Ciaranfi, N., D'Onofrio, S., 1977. Paleoclimatic record of a long deep-sea core from the eastern Mediterranean. Quat. Res. 8, 205–235.

Clemens, S.C., Tiedemann, R., 1997. Eccentricity forcing of Pliocene–Early Pleistocene climate revealed in a marine oxygen isotope record. Nature 385, 801–804.

Combourieu-Nebout, N., 1991. Late Pliocene northern Hemisphere glaciations: the continental and marine responses in the central Mediterranean. Quat. Sci. Rev. 10 (4), 319–334.

Combourieu-Nebout, N., Touron, J.L., Zahn, R., Capotondi, L., Londeix, L., Pahnke, K., 2002. Enhanced aridity and atmospheric high-pressure stability over the western Mediterranean during the North Atlantic cold events of the past 50 ky. Geology 30 (10), 863–866.

Corliss, B.H., 1985. Microhabitats of benthic foraminifera within deep-sea sediments. Nature 314, 435–438.

Cortijo, E., Labeyrie, L., Vidal, L., Vautravers, M., Chapman, M., Duplessy, J.-C., Elliot, M., Arnold, M., Turon, J.-L., Auffret, G., 1997. Changes in sea surface hydrology associated with Heinrich event 4 in the North Atlantic Ocean between 40 an 60°N. Earth Planet. Sci. Lett. 146, 29–45.

Curry, W.B., Oppo, D.W., 1997. Synchronous, high-frequency oscillations in tropical sea surface temperatures and North Atlantic deep water production during the last glacial cycle. Paleoceanography 12 (1), 1–14.

Dansgaard, W., Johnsen, S.J., Clausen, H.B., Dahl-Jensen, D., Gundestrup, N.S., Hammer, C.U., Hvidberg, C.S., Steffensen, J.P., Sveinbjörnsdottir, A.E., Jouzel, J., Bond, G., 1993. Evi-

dence for general instability of past climate from a 250-kyr ice-core record. Nature 364, 218–220.

de Rijk, S., Hayes, A., Rohling, E.J. (Eds.), 1999. Eastern Mediterranean Sapropel S1 Interruption: an Expression of the Onset of Climatic Deterioration around 7 ka BP, [Monograph] Fifth Decade of Mediterranean Paleoclimate and Sapropel Studies, vol. 153. Elsevier, Amsterdam. 337–343 pp.

deMenocal, P.B., Rind, D., 1993. Sensitivity of Asian and African monsoon climate to variations in seasonal insolation, glacial ice cover, sea surface temperature and Asian orography. J. Geophys. Res. 98 (D4), 7265–7287.

Dulac, F., Moulin, C., Lambert, C.E., Guillard, F., Poitou, J., Guelle, W., Quetel, C.R., Schneider, X., Ezat, U., 1996. Quantitative remote sensing of African dust transport to the Mediterranean. In: Chester, S.G.a.R. (Ed.), The Impact of Desert Dusts Across the Mediterranean, Environmental Science and Technology Library. Kluwer Academic Publishers, Dordrecht, pp. 25–49.

Emeis, K.-C., Robertson, A.H.F., Richter, C., 1996. Preliminary Report Mediterranean I. Ocean Drilling Program leg, vol. 160.

Emeis, K.-C., Schulz, H., Struck, U., Rossignol-Strick, M., Erlenkeuser, H., Howell, M.W., Kroon, D., Mackensen, A., Ishizuka, S., Oba, T., Sakamoto, T., Koizumi, I., 2003. Eastern Mediterranean surface water temperatures and $d^{18}O$ composition during sapropel formation in the Late Quaternary. Paleoceanography 18 (1), 1–18.

Fariduddin, M., Loubere, P., 1997. The surface ocean productivity response of deeper water benthic foraminifera in the Atlantic Ocean. Mar. Micropaleontol. 32, 289–310.

Foucault, A., Mélières, F., 1995. Nature et origine des cycles sedimentaires metriques du Pliocene de l'Ouest mediterraneen d'apres l'etude du contenu terrigene de la Formation Narbone (Punta Piccola, Sicile, Italie). C. R. Acad. Sci. Paris t. 321 (serie lla), 869–876.

Foucault, A., Mélières, F., 2000. Palaeoclimatic cyclicity in central Mediterranean Pliocene sediments: the mineralogical signal. Palaeogeog. Palaeoclimatol. Palaeoecol. 158, 311–323.

Giorgi, F., 1996. Climate modelling over the Mediterranean region. In: Guerzoni, S., Roy, C. (Eds.), The Impact of Desert Dust Across the Mediterranean, Environmental Science and Technology Library. Kluwer, Dordrecht, pp. 1–14.

Guerzoni, S., Roy, C., 1996. The impact of desert dust across the Mediterranean. Environmental Science and Technology Library, vol. 11. Kluwer, Dordrecht. 389 pp.

Gupta, A.K., 1997. Paleoceanographic and paleoclimatic history of the Somali Basin during the Pliocene–Pleistocene: multivariate analyses of benthic foraminifera from DSDP Site 241 (Leg 25). J. Foraminiferal Res. 27 (3), 196–208.

Hagelberg, T.K., Bond, G., deMenocal, P., 1994. Milankovitch band forcing of sub-Milankovitch climate variability during the Pleistocene. Paleoceanography 9 (4), 545–558.

Harloff, J., Mackensen, A., 1997. Recent benthic foraminiferal associations and ecology of the Scotia Sea and Argentine Basin. Mar. Micropaleontol. 31, 1–29.

Hayward, B.W., Neil, H., Carter, R., Grenfell, H.R., Hayward, J., 2002. Factors influencing the distribution patterns of recent deep-sea benthic foraminifera, east of New Zealand, Southwest Pacific Ocean. Mar. Micropaleontol. 46, 139–176.

Heinrich, H., 1988. Origin and consequences of cyclic ice rafting in the NE Atlantic Ocean during the past 130,000 years. Quat. Res. 29, 142–152.

Hemleben, C., Spindler, M., Anderson, O.R., 1989. Modern Planktonic Foraminifera. Springer Verlag, New York.

Hilbrecht, H., 1996. Extant planktic foraminifera and the physical environment in the Atlantic and Indian Oceans. Mitt. Geol. Inst. EidgenoÉss. Tech. Hochsch. Univ. ZuÉr. 300 (Neue Folge). 93 pp.

Hilgen, F.J., 1991a. Astronomical calibration of Gauss to Matuyama sapropels in the Mediterranean and implication for the geomagnetic polarity time scale. Earth Planet. Sci. Lett. 104, 226–244.

Hilgen, F.J., 1991b. Extension of the astronomically calibrated (polarity) time scale to the Miocene/Pliocene boundary. Earth Planet. Sci. Lett. 107, 349–368.

Hilgen, F.J., Lourens, L.J., Berger, A., Loutre, M.F., 1993. Evaluation of the astronomically calibrated time scale for the Late Pliocene and earliest Pleistocene. Paleoceanography 8 (5), 549–565.

Hilgen, F.J., Krijgsman, W., Langereis, C.G., Lourens, L.J., Santarelli, A., Zachariasse, W.J., 1995. Extending the astronomical (polarity) time scale into the Miocene. Earth Planet. Sci. Lett. 136, 495–510.

Imbrie, J., Imbrie, J.Z., 1980. Modelling the climatic response to orbital variations. Science 207, 943–952.

Imbrie, J., Hays, J.D., Martinson, D.G., McIntyre, A., Mix, A.C., Morley, J.J., Pisias, N.G., Prell, W.L., Shackleton, N.J., 1984. The orbital theory of Pleistocene climate: support from a revised chronology of the marine $d^{18}O$ record. In: Berger, A., Imbrie, J., Hays, J., Kukla, G., Saltzman, B. (Eds.), Milankovitch and Climate, Understanding the Response to Astronomical Forcing, NATO Advanced Science Institute Series. DReidel Publishing Company, Dordrecht, p. 510.

Imbrie, J., Boyle, E.A., Clemens, S.C., Duffy, A., Howard, W.R., Kukla, G., Kutzbach, J., Martinson, D.G., McIntyre, A., Mix, A., Molfino, B., Morley, J., Pisias, N., Prell, W.L., Raymo, M.E., Shackleton, N.J., Toggweiler, J.R., 1992. On the structure and origin of major glaciation cycles: 1. Linear response to Milankovitch forcing. Paleoceanography 7, 701–738.

Imbrie, J., Mix, A.C., Martinson, D.G., 1993. Milankovitch theory viewed from Devils Hole. Nature 363, 531–533.

Jannink, N.T., Zachariasse, W.J., Van der Zwaan, G.J., 1998. Living (Rose Bengal stained) benthic foraminifera from the Pakistan continental margin (northern Arabian Sea). Deep-Sea Res., I 45, 1483–1513.

Jian, Z., Wang, L., Kienast, M., Sarnthein, M., Kuhnt, W., Lin, H., Wang, P., 1999. Benthic foraminiferal paleoceanography of the South China Sea over the last 40,000 years. Mar. Geol. 156, 159–186.

Jorissen, F.J., Barmawidjaja, D.M., Puskaric, S., Van der Zwaan, G.J., 1992. Vertical distribution of benthic foraminifera in the northern Adriatic Sea: the relation with the organic flux. Mar. Micropaleontol. 19, 131–146.

Kallel, N., Paterne, M., Duplessy, J.-C., Vergnaud-Grazzini, C., Pujol, C., Labeyrie, L., Arnold, M., Fontugne, M., Pierre, C., 1997a. Enhanced rainfall in the Mediterranean region during the last sapropel event. Oceanol. Acta 20 (5), 697–712.

Kallel, N., Paterne, M., Labeyrie, L., Duplessy, J.-C., Arnold, M., 1997b. Temperature and salinity records in the Tyrrhenian Sea during the last 18,000 years. Palaeogeog. Palaeoclimatol. Palaeoecol. 135, 97–108.

Kallel, N., Duplessy, J.C., Labeyrie, L., Fontugne, M., Paterne, M., Montacer, M., 2000. Mediterranean pluvial periods and sapropel formation over the last 200 000 years. Palaeogeog. Palaeoclimatol. Palaeoecol. 157 (1–2), 45–58.

Keeling, C.D., Whorf, T.P., 2000. The 1800-year oceanic tidal cycle: a possible cause of rapid climate change. PNAS 97, 3814–3819.

Kennett, J.P., Srinivasan, M.S., 1983. Neogene Planktonic Forminifera. Hutchinson Ross Publishing, Pennsylvania. 263 pp.

Kroon, D., Alexander, I., Little, M., Lourens, L.J., Matthewson, A., Robertson, A.H.F., Sakamoto, T., 1998. Oxygen isotope and sapropel stratigraphy in the eastern Mediterranean during the last 3.2 million years. In: Robertson, A.H.F., Emeis, K.-C., Richter, C., Camerlenghi, A. (Eds.), Proceedings of the Ocean Drilling Program, Scientific ResultsOcean Drilling Program, College Station, TX, pp. 181–190.

Kuhnt, W., Hess, S., Jian, Z., 1999. Quantitative composition of benthic foraminiferal assemblages as a proxy indicator for carbon flux rates in the South China Sea. Mar. Geol. 156, 123–158.

Laskar, J., Joutel, F., Boudin, F., 1993. Orbital, precessional, and insolation quantities for the Earth from −20 Myr to +10 Myr. Astron. Astrophys. 270, 522–533.

Laskar, J., Robutel, P., Joutel, F., Gastineau, M., Correia, A.C.M., Levrard, B., 2004. A long term numerical solution for the insolation quantities of the Earth. Astron. Astrophys. 428, 261–285.

Le Treut, H., Ghil, M., 1983. Orbital forcing, climatic interactions, and glaciation cycles. J. Geophys. Res. 93, 9365–9383.

Lisiecki, L.E., Raymo, M.E., 2005. A Pliocene–Pleistocene stack of 57 globally distributed benthic $d^{18}O$ records. Paleoceanography 20, 1003.

Liu, H.-S., 1992. Frequency variations of the Earth's obliquity and the 100-kyr ice-age cycles. Nature 358, 397–399 (30 July).

Liu, H.-S., 1995. A new driving mechanism of Milankovitch glaciation cycles. Earth Planet. Sci. Lett. 131, 17–26.

Loubere, P., Moss, K., 1986. Late Pliocene climatic change and the onset of Northern Hemisphere glaciation as recorded in the northeast Atlantic Ocean. Geol. Soc. Amer. Bull. 77, 818–828.

Lourens, L.J., Hilgen, F.J., Gudjonsson, J., Zachariasse, W.J., 1992. Late Pliocene to Early Pleistocene astronomically-forced sea surface productivity and temperature variations in the Mediterranean. Mar. Micropaleontol. 19, 49–78.

Lourens, L.J., Antonarakou, A., Hilgen, F.J., Van Hoof, A.A.M., Vergnaud-Grazzini, C., Zachariasse, W.J., 1996. Evaluation of the Plio–Pleistocene astronomical timescale. Paleoceanography 11 (4), 391–413.

Lourens, L.J., Hilgen, F.J., Raffi, I., 1998. Base of large Gephyrocapsa and astronomical calibration of Early Pleistocene sapropels in site 967 and hole 969D: solving the chronology of the Vrica section (Calabria, Italy). Proceedings of the Ocean Drilling Program, Scientific Results, vol. 160, pp. 191–197.

Lourens, L.J., Wehausen, R., Brumsack, H.J., 2001. Geological constraints on tidal dissipation and dynamical ellipticity of the Earth over the past three million years. Nature 409, 1029–1032.

Lourens, L.J., Hilgen, F.J., Shackleton, N.J., Laskar, J., Wilson, D., 2004. The Neogene Period. In: Gradstein, F., Ogg, I., Smith, A. (Eds.), A Geologial Timescale 2004. Cambridge University Press, UK.

Lutze, G.F., Colbourn, W.T., 1984. Recent benthic foraminifera from the continental margin of northwest Africa: community structure and distribution. Mar. Micropaleontol. 8, 361–401.

MacAyeal, D.R., 1993. Binge/purge oscillations of the Laurentide ice sheet as a cause of the North Atlantic's Heinrich events. Paleoceanography 8, 775–784.

Mackensen, A., Sejrup, H.P., Jansen, E., 1985. The distribution of benthic foraminifera on the continental slope and rise off Norway. Mar. Micropaleontol. 9, 275–306.

Mackensen, A., Füttere, D.K., Grobe, H., Schmiedl, G., 1993. Benthic foraminiferal assemblages from the eastern South Atlantic Polar Front region between 35 and 57°S: distribution, ecology and fossilization potential. Mar. Micropaleontol. 22, 33–69.

Mackensen, A., Schmiedl, G., Harloff, J., Giese, M., 1995. Deep-sea foraminifera in the South Atlantic Ocean: ecology and assemblage generation. Micropaleontology 41 (4), 342–358.

Martinson, D.G., Pisias, N.G., Hays, J.D., Imbrie, J., Moore, T.C., Shackleton, N.J., 1987. Age dating and the orbital theory of the Ice Ages: development of a high-resolution 0 to 300,000-year chronostratigraphy. Quat. Res. 27, 1–29.

McIntyre, A., Molfino, B., 1996. Forcing of Atlantic equatorial and subpolar millenial cycles by precession. Science 274, 1867–1870.

McIntyre, K., Delaney, M.L., Ravelo, A.C., 2001. Millenial-scale climate change and oceanic processes in the Late Pliocene and Early Pleistocene. Paleoceanography 16 (5), 535–543.

Meggers, H., Baumann, K.-H., 1997. Contributions to the Micropaleontology and Paleceanography of the Northern North Atlantic. In: Hass, H.C., Kaminski, M.A. (Eds.), Grzybowski Foundation Special Publication, pp. 39–50.

Miao, Q., Thunell, R.C., 1996. Late Pleistocene–Holocene distribution of deep-sea benthic foraminifera in the South China Sea and Sulu Sea: paleoceanographic implications. J. Foraminiferal Res. 26 (1), 9–23.

Moreno, A., Targarona, J., Henderiks, J., Canals, M., Freudenthal, T., Meggers, H., 2001. Orbital forcing of dust supply to the North Canary Basin over the last 250 kyr. Quat. Sci. Rev. 20, 1327–1339.

Moreno, A., Cacho, I., Canals, M., Grimalt, J.O., Sanchez-Vidal, A., 2004. Millenial-scale variability in the productivity signal from the Alboran Sea record, Western Mediterranean Sea. Palaeogeog. Palaeoclimatol. Palaeoecol. 211, 205–219.

Murray, J.W., 1991. Ecology and Palaeoecology of Benthic Foraminifera. Longman Scientific and Technical. 397 pp.

Negri, A., Capotondi, L., Keller, J., 1999. Calcareous nannofossils, planktonic foraminifera and oxygen isotopes in the Late Quaternary sapropels of the Ionian Sea. Mar. Geol. 157, 89–103.

O'Neil, J.R., Clayton, R.N., Mayeda, T.K., 1969. Oxygen isotope fractionation in divalent metal carbonates. J. Chem. Phys. 52, 5547–5558.

Oerlemans, J., van der Veen, C.J., 1984. Ice Sheets and Climate. Kluwer Academic, Hingham, Mass. 217 pp.

Ortiz, J., Mix, A., Harris, S., O'Connell, S., 1999. Diffuse spectral reflectance as a proxy for percent carbonate content in the North Atlantic sediments. Palaeoceanography 14 (2), 171–186.

Paterne, M., Kallel, N., Labeyrie, L., Vautravers, M., Duplessy, J.-C., Rossignol-Strick, M., Cortijo, E., Arnold, M., Fontugne, M., 1999. Hydrological relationship between the North Atlantic Ocean and the Mediterranean Sea during the past 15–75 kyr. Paleoceanography 14 (5), 626–638.

Perry, C.A., Hsu, K.J., 2000. Geophysical, archaeological, and historical evidence support a solar-output model for climate change. PNAS 97, 12433–12438.

Pestiaux, P., Mersch, I.v.d., Berger, A., Duplessy, J.C., 1988. Paleoclimatic variability at frequencies ranging from 1 cycle per 10,000 years to 1 cycle per 1000 years: evidence for nonlinear behaviour of the climate system. Clim. Change 12, 9–37.

Pinardi, N., Masetti, E., 2000. Variability of the large scale general circulation of the Mediterranean Sea from observations and modelling: a review. Palaeogeog. Palaeoclimatol. Palaeoecol. 158, 153–173.

Poore, R.Z., Berggren, W.A., 1975. The morphology and classification of *Neogloboquadrina atlantica* (Berggren). J. Foraminiferal Res. 5, 692–694.

Prospero, J.M., 1996. Saharan dust transport over the North Atlantic Ocean and Mediterranean. In: Guerzoni, S., Roy, C. (Eds.), The Impact of Desert Dust Across the Mediterranean, Environmental Science and Technology Library. Kluwer, Dordrecht, pp. 133–152.

Qvale, G., 1986. Distribution of benthic foraminifera in surface sediments along the Norwegian continental slope shelf between 62 and 72°N. Nor. Geol. Tidsskr. 66, 209–221.

Rathburn, A.E., Corliss, B.H., 1994. The ecology of living (stained) benthic foraminifera from the Sulu Sea. Paleoceanography 9 (1), 87–150.

Raymo, M.E., Ruddiman, W.F., Backman, J., Clement, B.M., Martinson, D.G., 1989. Late Pliocene variation in northern hemisphere ice sheets and North Atlantic deep water circulation. Palaeoceanography 4, 413–446.

Raymo, M.E., Hodell, D., Jansen, E., 1992. Response of deep ocean circulation to initiation of northern hemisphere glaciation (3–2 Ma). Paleoceanography 7, 645–672.

Rial, J.A., 1999. Pacemaking of the ice ages by frequency modulation of earth's orbital eccentricity. Science 285, 564–571.

Rio, D., Sprovieri, R., Di Stefano, E., 1994. The Gelasian stage: a proposal of a new chronostratigraphic unit of the Pliocene series. Riv. Ital. Paleontol. Stratigr. 100 (1), 103–124.

Rohling, E.J., Gieskes, W.W.C., 1989. Late Quaternary changes in Mediterranean intermediate water density and formation rate. Paleoceanography 5, 531–545.

Rohling, E.J., Hilgen, F.J., 1991. The eastern Mediterranean climate at times of sapropel formation: a review. Geol. Mijnb. 70, 252–264.

Rohling, E.J., Jorissen, F.J., Vergnaud-Grazzini, C., Zachariasse, W.J., 1993. Northern Levantine and Adriatic quaternary planktic foraminifera: reconstruction of paleoenvironmental gradients. Mar. Micropaleontol. 21, 191–218.

Rohling, E.J., Hayes, A., De Rijk, S., Kroon, D., Zachariasse, W.J., Eisma, D., 1998. Abrupt cold spells in the northwest Mediterranean. Paleoceanography 13, 316–322.

Rohling, E.J., Sprovieri, R., Cane, T., Casford, J.S.L., Cooke, S., Bouloubassi, I., Emeis, K.-C., Schiebel, R., Rogerson, M., Hayes, A., Jorissen, F.J., Kroon, D., 2004. Reconstructing past planktic foraminiferal habitats using stable isotope data: a case history for Mediterranean sapropel S5. Mar. Micropaleontol. 50, 89–123.

Rossignol-Strick, M., 1983. African monsoons, an immediate climate response to orbital insolation. Nature 304, 46–49.

Rossignol-Strick, M., 1985. Mediterranean Quaternary sapropels, an immediate response of the African monsoon to variation of insolation. Palaeogeog. Palaeoclimatol. Palaeoecol. 49, 237–263.

Rossignol-Strick, M., Nesteroff, W., Olive, P., Vergnaud-Grazzini, C., 1982. After the deluge: Mediterranean stagnation and sapropel formation. Nature 295, 105–110.

Ruddiman, W.F., McIntyre, A., Raymo, M., 1986. Matuyama 41,000-year cycles: North Atlantic Ocean and northern hemisphere ice sheets. Earth Planet. Sci. Lett. 80, 117–129.

Ruddiman, W.F., Raymo, M.E., Martinson, D.G., Clement, B.M., Backman, J., 1989. Pleistocene evolution of northern hemisphere climate. Paleoceanography 4, 353–412.

Sakamoto, T., Janecek, T., Emeis, K.-C., 1998. Continuos sedimentary sequences from the eastern Mediterranean Sea: composite depth sections. In: Robertson, A.H.F., Emeis, K.-C., Richter, C., Camerlenghi, A. (Eds.), Proceedings of the Ocean Drilling Program, Scientific Results. ODP, College Station, Texas, pp. 37–51.

Saltzman, B., Sutera, A., 1984. A model of the internal feedback system involved in Late Quaternary climatic variations. J. Atmos. Sci. 41 (5), 736–745.

Sanchez-Goni, M.F., Cacho, I., Turon, J.L., Guiot, J., Sierro, F.J., Peypouquet, J.-P., Grimalt, J.O., Shackleton, N.J., 2002. Synchroneity between marine and terrestrial responses to millennial scale climatic variability during the last glacial period in the Mediterranean region. Clim. Dyn. 19, 95–105.

Schiebel, R., Waniek, J., Bork, M., Hemleben, C., 2001. Planktic foraminiferal production stimulated by chlorophyll redistribution and entrainment of nutrients. Deep-Sea Res., I 48, 721–740.

Schmidt, G.A., Mulitza, S., 2002. Global calibration of ecological models for planktic foraminifera from coretop carbonate oxygen-18. Mar. Micropaleontol. 44, 125–140.

Schmiedl, G., Mackensen, A., Müller, P.J., 1997. Recent benthic foraminifera from the eastern South Atlantic Ocean: dependence on food supply and water masses. Mar. Micropaleontol. 32, 249–287.

Schmiedl, G., Mitschele, A., Bec, S., Emeis, K.-C., Hemleben, C., Schulz, H., Sperling, M., Weldeab, S., 2003. Benthic foraminiferal record of ecosystem variability in the eastern Mediterranean Sea during times of sapropel S5 and S6 deposition. Palaeogeog. Palaeoclimatol. Palaeoecol. 190, 139–164.

Seidenkrantz, M.-S., Kouwenhoven, T.J., Jorissen, F.J., Shackleton, N.J., Van der Zwaan, G.J., 2000. Benthic foraminifers as indi-

cators of changing Mediterranean–Atlantic water exchange in the Late Miocene. Mar. Geol. 163, 387–407.
Shackleton, N.J., 1967. Oxygen isotope analyses and Pleistocene temperatures reassessed. Nature 215, 15–17.
Shackleton, N.J., 1974. Attainment of isotopic equilibrium between ocean water and the benthonic foraminifera genus Uvigerina: isotopic changes in the ocean during the last glacial. Les Meth. Quant. d'étude Var. Clim. au Cour du Pleist., Coll. Int. C.N.R.S., vol. 219, pp. 203–209.
Shackleton, N.J., 2000. The 100,000-year Ice-Age cycle identified and found to lag temperature, carbon dioxide, and orbital eccentricity. Science 289, 1897–1902.
Shackleton, N.J., Backman, J., Zimmerman, H., Kent, D.V., Hall, M.A., Roberts, D.G., Schitker, D., Baldauf, J., 1984. Oxygen isotope calibration of the onset of ice-rafting and history of glaciation in the North Atlantic region. Nature 307, 620–623.
Shackleton, N.J., Berger, A., Peltier, W.R., 1990. An alternative astronomical calibration of the Lower Pleistocene timescale based on ODP site 677. Trans. R. Soc. Edinb. Earth Sci. 81, 251–261.
Shackleton, N.J., Hall, M.A., Pate, D., 1995. Pliocene stable isotope stratigraphy of ODP Site 846. Proc. Ocean Drill. Prog., Sci. Results 138, 337–355.
Short, D.A., Mengel, J.G., 1986. Tropical climatic phase lags and Earth's precession cycle. Nature 323, 48–50.
Short, D.A., Mengel, J.G., Crowley, T.J., Hyde, W.T., North, G.R., 1991. Filtering of Milankovitch cycles by earth's geography. Quat. Res. 35, 157–173.
Sprovieri, R., 1993. Pliocene–Early Pleistocene astronomically forced planktonic foraminifera abundance fluctuations and chronology of Mediterranean calcareous plankton bio-events. Riv. Ital. Paleontol. Stratigr. 99 (3), 371–414.
Sprovieri, R., Hasegawa, S., 1990. Plio–Pleistocene benthic foraminifer stratigraphic distribution in the deep-sea record of the Tyrrhenian Sea (OPD Leg 107). In: Kastens, K.A., Moscle, J., et al., (Eds.), Proceedings of the Ocean Drilling Program, Scientific Results. Ocean Drilling Program, College Station, TX, pp. 529–549.
Sprovieri, R., Thunell, R., Howell, M., 1986. Paleontological and geochemical analysis of three laminated sedimentary units of Late Pliocene–Early Pleistocene age from the Monte San Nicola section in Sicily. Riv. Ital. Paleontol. Stratigr. 92 (3), 401–434.
Steenbrink, J., Kloosterboer van Hoeve, M.L., Hilgen, F.J., 2003. Millennial-scale climate variations recorded in Early Pliocene colour reflectance time series from the lacustrine Ptolemais Basin (NW Greece). Glob. Planet. Change 36 (1–2), 47–75.
Stott, L., Poulsen, C., Lund, S., Thunell, R., 2002. Super ENSO and global climate oscillations at millenial time scales. Science 297, 2345–2348.
Thunell, R., Williams, D.F., 1989. Glacial–Holocene salinity changes in the Mediterranean Sea: hydrographic and depositional effects. Nature 338, 493–496.
Tuenter, E., Weber, S.L., Hilgen, F.J., Lourens, L.J., Ganopolski, A., 2005. Simulation of climate phase lags in respond to precession and obliquity forcing. Clim. Dyn. 24 (2–3), 279–295.
Van Geel, B., Raspopov, O.M., Renssen, H., van der Plicht, J., Dergachev, V.A., Meijer, H.A.J., 1999. The role of solar forcing upon climate change. Quat. Sci. Rev. 18, 331–338.
van Os, B.J.H., Lourens, L.J., Beaufort, L., Hilgen, F.J., de Lange, G.J., 1994. The formation of Pliocene sapropels and carbonate cycles in the Mediterranean: diagenesis, dilution and productivity. Paleoceanography 9, 601–617.
Vergnaud-Grazzini, C., Ryan, W.B.F., Cita, M.B., 1977. Stable isotope fractionation, climatic change and episodic stagnation in the eastern Mediterranean during the Late Quaternary. Mar. Micropaleontol. 2, 353–370.
Verhallen, P.J.J.M., 1987. Early development of *Bulimina marginata* in relation to paleo-environmental changes in the Mediterranean Pliocene. Kon. Ned. Akad. Wet., B 90, 161–180.
Verhallen, P.J.J.M., 1991. Late Pliocene to Early Pleistocene Mediterranean mud-dwelling foraminifera: influence of a changing environment on community structure and evolution. Utrecht Micropaleontol. Bull. 40 (220 pp.).
Wara, M.W., Ravelo, A.C., Revenaugh, J.S., 2000. The pacemaker always rings twice. Paleoceanography 15 (6), 616–624.
Wehausen, R., 1999. Anorganische Geochemie zyklischer Sedimente aus dem östlichen Mittelmeer: Rekonstruktion der Paläoumweltbedingungen. Dissertation Thesis, Carl-von-Ossietzky-Universität, Oldenburg, 162 pp.
Wehausen, R., Brumsack, H.-H., 1999. Cyclic variations in the chemical composition of eastern Mediterranean Pliocene sediments: a key for understanding sapropel formation. Mar. Geol. 153, 161–176.
Willis, K.J., Kleczkowski, A., Briggs, K.M., Gilligan, C.A., 1999. The role of sub-Milankovitch climatic forcing in the initiation of the northern hemisphere glaciation. Science 285, 568–571.
Zachariasse, W.J., Gudjonsson, L., Hilgen, F.J., Lourens, L.J., Verhallen, P.J.J.M., Langereis, C.G., Zijderveld, J.D.A., 1990. Late Gauss to Early Matuyama invasions of *Neogloboquadrina atlantica* in the Mediterranean and associated record of climatic change. Paleoceanography 5, 239–252.
Zijderveld, J.D.A., Hilgen, F.J., Langereis, C.G., Verhallen, P.J.J.M., Zachariasse, W.J., 1991. Integrated magnetostratigraphy and biostratigraphy of the Upper Pliocene–Lower Pleistocene from the Monte Singa and Crotone areas Calabria (Italy). Earth Planet. Sci. Lett. 107, 697–714.